universität wien

MASTERARBEIT / MASTER'S THESIS

Titel der Masterarbeit / Title of the Master 's Thesis

Effect of the arginase inhibitor nor-NOHA on markers of intestinal permeability in aging mice

verfasst von / submitted by

Ena Tesic, BSc

angestrebter akademischer Grad / in partial fulfilment of the requirements for the degree of

Master of Science (MSc)

Wien, 2021 / Vienna, 2021

Studienkennzahl lt. Studienblatt / degree programme code as it appears on the student record sheet:	UA 066 838
Studienrichtung lt. Studienblatt / degree programme as it appears on the student record sheet:	Masterstudium Ernährungswissenschaften
Betreut von / Supervisor:	Univ.-Prof. Dr. Ina Bergheim

Content

I. List of abbreviations

ACTB	β-Actin
AICAR	5-Aminoimidazole-4-carboxamide riboside
AJ	Adherens junction
AMPK	Adenosine monophosphate-activated protein kinase
APS	Ammonium persulfate
Aq. dest.	Distilled water
BSA	Bovine serum albumin
cDNA	Complementary deoxyribonucleic acid
DALY	Disability-adjusted life year
DTT	Dithiothreitol
GI	Gastrointestinal
HMGB1	High mobility group box-1 protein
IgA	Immunoglobulin A
KRH buffer	Krebs-Henseleit bicarbonate buffer
L-NOHA	N-hydroxy-L-arginine
MMP	Nonfat dried milk powder
mRNA	Messenger ribonucleic acid
MW	Mean
MYLK	Myosin light-chain kinase
NO	Nitric oxide
nor-NOHA	N-ω-Hydroxy-L-norarginine
NOS	Nitric oxide synthase
OD Unit	Optical density unit
Occ	Occludin
pOcc	Phospho-occludin

PVDF	Polyvinylidene fluoride
qPCR	Quantitative polymerase chain reaction
RhoA	Ras homolog gene family, member A
ROCK	Rho-associated protein kinase
rRNA	Ribosomal ribonucleic acid
SDS	Sodium dodecyl sulphate
SEM	Standard error of the mean
TBE buffer	TRIS/Borate/ Ethylenediaminetetraacetic acid buffer
TBS	Tris-buffered saline
TBST	Tris-buffered saline/Tween 20
TEMED	N,N,N',N'-tetramethylethane-1,2-diamine
TJ	Tight junction
TRIS	Trisaminomethane
YLDs	Years lived with disability
YLLs	Years of life lost
ZO-1	Zonula occludens-1

II. List of tables

III. List of figures

1. Introduction

1.1. Aging: Definition and demographic development as well as impairments and decline associated with aging

Definition

Aging can be defined as the changes in an organism associated with the passing of time, between development including growth, maturation and senescence until death [1]. The process of aging is associated in numerous types of physiological deterioration, affecting systemic, mechanical, structural, and functional changes, subsequently leading to altered tissue and hormones responses, as well as growing vulnerability, altered body composition, psychosocial deficits, et cetera [2]. Fundamental aging processes e.g., low-grade inflammation, macromolecular and organelle dysfunction and stem cell dysfunction, are frequent at sites of age-related pathogenesis [88].

Age represents a major risk factor for noncommunicable chronic pathologies [105], such as neurodegenerative, cardiovascular, chronic obstructive pulmonary and gastrointestinal diseases, cancer, diabetes, kidney dysfunction, osteoarthritis, frailty, immobility, blindness and numerous other disorders [87] [89]. Ultimately these subclinical and clinical health modulations acuminate, even with the coexistence of two or more conditions, and pose an age related multimorbidity problem [3].

Demographic development

Globally, the population aged 60 and over is growing faster than all other age groups, and today the number of people aged 60 years and older has outnumber children younger than 5 years [5]. The elderly population is living longer: to be more precise, according to the World Health Organisation, in 2019 the population aged 60 years and older was 1 billion. Predictions are that the number of aged people will increase in coming decades, accelerating by 2030 to 1.4 billion and by 2050 to 2.1 billion [85]. The change in demography, shift in distribution of a country's population towards older ages, is a global challenge [104]. It started in high-income countries, but now low- and middle-income countries are experiencing a shift alike [4].

The disability-adjusted life year (DALY) is an evaluating measure of global or regional disease burden. It is expressed as the sum of years lost due premature mortality, years of life lost (YLLs), and due to ill-health, years lived with disability (YLDs) [7].

In 2018, the number of healthy life years at birth was estimated for women at 57.0 years and for men at 56.8 years, in Austria. This represents approximately 68% and 72% of the total life expectancy [8].

Unhealthy lifestyle, such as obesity, lack of exercise, smoking or alcohol abuse, are getting more common and have costly consequences, especially later in life [106]. Preventive strategies that promote healthy aging are critical, not just the expanding of life expectancy [6]. Unhealthy aging places great financial pressure on the health system, increases health care expenditures and poses a major public health burden, as it is one of the leading risk factors for most chronic diseases which have high associated costs of medical services and supplies, diagnosis, drugs, treatment, and care [86] [103].

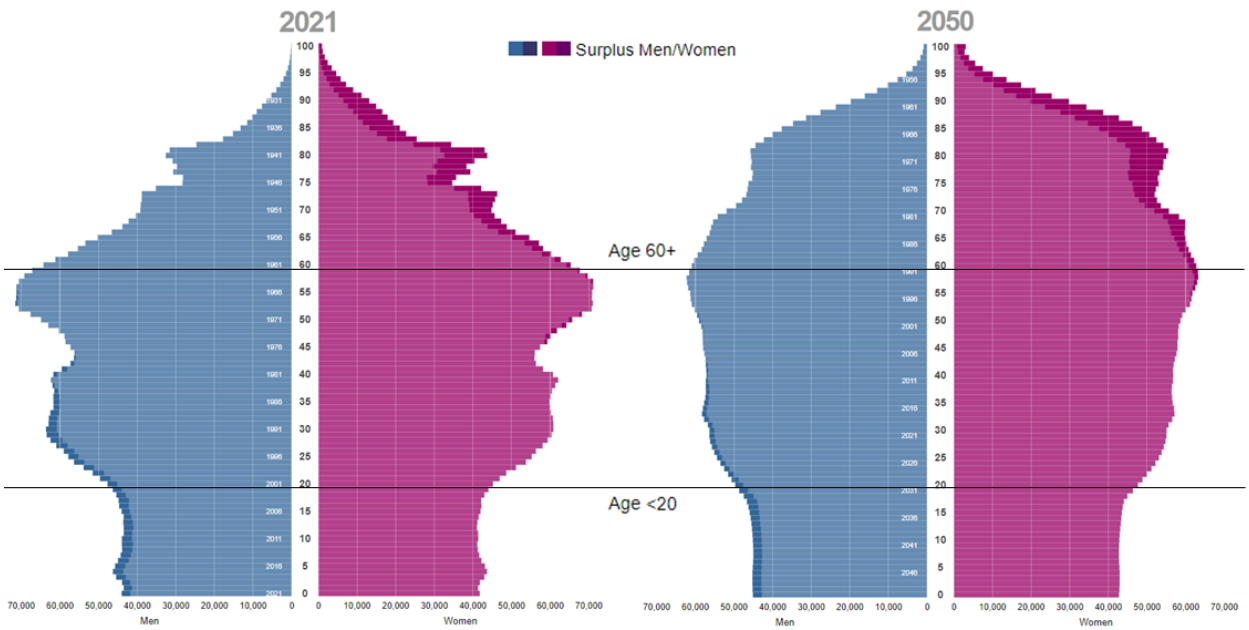

Age	Population	Pct.
60+	2,334,577	26%
20–59	4,896,810	55%
<20	1,729,466	19%
Total	8,960,853	100%

Age	Population	Pct.
60+	3,257,567	34%
20–59	4,569,841	48%
<20	1,778,518	19%
Total	9,605,926	100%

Figure 1: Predicted demographic development in Austria from the year 2021 to 2050.
(Modified from STATISTIK AUSTRIA, Bevölkerung nach Alter und Geschlecht) [90]

Impairments and decline associated with aging

Principal characteristic of aged organisms is the accumulation of cellular senescence, a permanent state of the cell cycle arrest [87] as response to various damaging stimuli [107]. During development and after injury, cellular senescence stimulates tissue remodelling, but it also contributes to inflammation, regenerative potential and function decline of tissues and tumorigenesis in aged organisms [108]. Excessive and aberrant accumulation of senescent cells in tissues affect negatively the regenerative capacities and create a proinflammatory milieu favourable for the onset and progression of various age-related phenotypes and pathologies [109] [110]. Aging research focuses on identifying aging phenotypes and investigation of underling complex genetic pathways, processes, and networks [12]. Damaging roles of senescent cells are potentially potent targets for antiaging approaches [111]. An ameliorated lifespan, associated with slowed aging and absence of disease, can be extended with genetic, environmental, health and pharmacological interventions in humans [9].

1.2. The gastrointestinal tract: Function and structure

Function

The gastrointestinal (GI) tract is the largest contact area in the body with environmental factors [150]. The overall function of the GI system is to digest ingested food, liquids, and drugs, through complex processes of digestive enzyme secretion, and absorption of nutrients. It also serves as a barrier against ingested pathogens and is central to human nutrition, health, and wellbeing [13] [14].

The selective and highly regulated passage of intestinal luminal contents is known as the intestinal barrier function. It has a dual role: the absorption of nutrients, water, and electrolytes from the lumen into the circulation, and the restriction of permeation of noxious luminal substances and microorganisms [46]. An intact intestinal barrier prevents the permeability of pathogens, endotoxins, antigens and proinflammatory substances into the body, while disintegrity can cause systemic inflammation and diseases [47]. Intestinal permeability indicates the mucosal barrier integrity and describes the paracellular leakiness of the intestinal lining [48].

Structure

The GI tract is composed of a series of layers, accomplishing the digestive function in a coordinated manner [19] (Figure 2.). Facing the intestinal lumen, a wide range of microorganisms, including bacteria, fungi, virus and parasites, are covering the mucus [26]. The colonization of the GI tract with gut microbiota is not only important for the metabolism of nutrients, but it has a crucial role in the development of a fully functional immune system [27]. The intestinal barrier is strongly dependent of the gut microbiome and its communication with the cells of the immune system and epithelial cells, because the interaction shapes specific responses to antigens, effector immune functions and balancing tolerance [25]. Next part of the intestinal barrier is the mucosal layer, which serves as protection of the absorptive and secretory epithelial cells, from pathogens, acids and digestive enzymes [22]. Large glycoproteins called mucins are major building blocks that give the mucus its properties [112]. Mucus serves multiple defence mechanisms, such as the innate immune system, antimicrobial mucus secretion, antioxidants, and epithelial intercellular tight junctions [23].
The physical components of the barrier, alongside the mucus layer and commensal microbiota, include the intestinal epithelium composed of different cell types. Enterocytes as the most abundant - which control the selective uptake, and goblet cells responsible for the secretion of mucus [50]. The immunological barrier elements consist of antimicrobial peptides secreted by Paneth cells and cellular immunity, such as secretory immunoglobulin A (IgA), lymphocytes, dendritic cell, etc. [49]. The remaining GI tract layers include the submucosal layer (containing nerves, lymphatics, connective tissue) and the smooth muscle layer (composed of longitudinal and circular smooth muscle) [21]. Luminal content moves along the GI tract via smooth muscle peristalsis, which ensures adequate exposure to the absorptive epithelial mucosal surface [24].

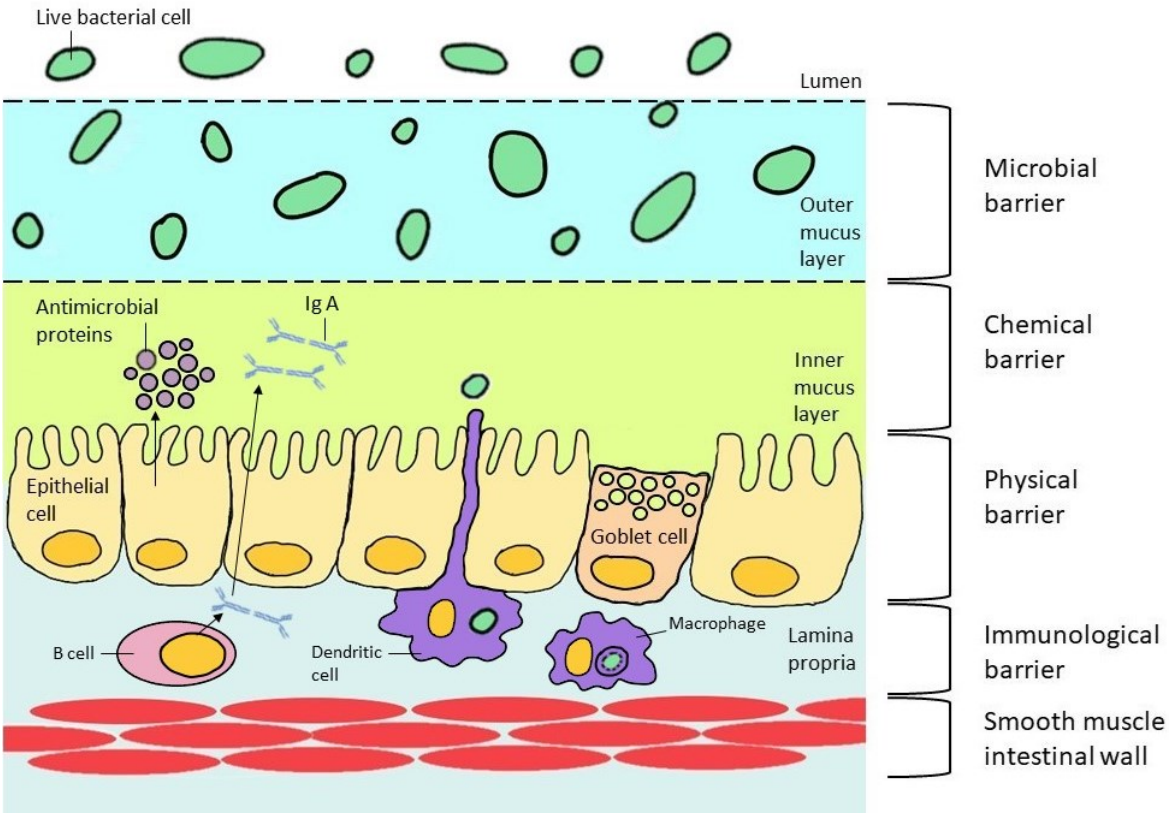

Figure 2: Schematic illustration of the intestinal barrier. *Commensal bacteria from the lumen inhibits pathogen colonization of the mucosa together with the mucus layer. Enterocytes, the prime absorptive epithelial cell type, regulate the absorption of luminal content. Various immune cells, of which some are immersed in the epithelium, detect changes in luminal microbial composition and respond by secreting antimicrobial proteins and immunoglobulins.* [28]

Depending on the characteristics of the luminal products (e.g., size, hydrophobicity) there are two routes of transport: the transcellular (predominantly mediated by specific transporters or channels located on the apical and basolateral membranes) and the paracellular pathway (precisely regulated by intercellular tight junction structures) [20] [51]. Tight junction proteins represent the rate-limiting step of paracellular transport and are responsible for the cell-to-cell adhesion [39]. Transmembrane proteins, including claudins, occludin, zonula occludens (ZO-1) and F-actin filaments, interact and form a highly integrated structure [94] (Figure 3.). Adherens junction (AJ) molecules, important for the assembly and function of TJs, are placed just below the TJ complex. Both TJs and AJs are supported by a perijunctional ring of actin and myosin. Further strength and sealing of the adhesion bonds, between adjacent intestinal epithelial cells, is accomplished by the desmosome [40] [52].

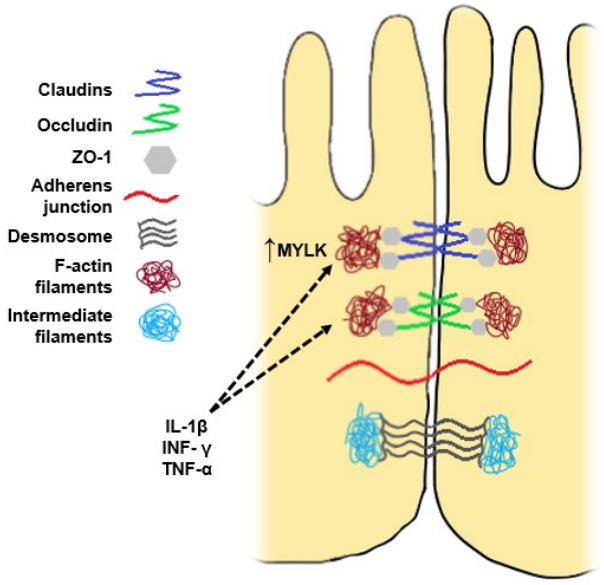

Figure 3: Schematic illustration of the intercellular junctional complex. *The intestinal epithelial cells are sealed by tight junction proteins such as claudins, occludin and ZO-1 preventing paracellular passage. Adherens junction influences the assembly and function of TJ proteins, whereas desmosome strengthens the sealing. In ageing, elevated levels of inflammatory cytokines (IL-1β, IFN-γ or TNF-α) can affect the integrity and permeability of the intestinal barrier by triggering myosin light chain kinase (MYLK) activity, thus remodelling the TJs at the perijunctional actomyosin cytoskeleton level.* [95] [96]

A single layer of epithelial cells separates the luminal content from immune cells in the lamina propria and the body's internal milieu [29]. Breaching this layer of epithelium by disruption of the TJ barrier function, leading to an increased paracellular permeability, results as the uptake of food antigens, proinflammatory molecules and entire, viable microorganisms, known as intestinal bacterial translocation [54]. Intestinal barrier disfunction is dynamically regulated by various extracellular stimuli, and is critically relevant in the pathogenesis of several pathologies [30] [53].

In recent years, the role of intestinal barrier function has gained more significance. Indeed, a compromised intestinal barrier function is reliably associated with a variety of clinical conditions, both intestinal (e.g., inflammatory bowel disease, celiac disease, irritable bowel syndrome and colorectal cancer) and systemic diseases, or diseases involving other organ systems (e.g., type I diabetes, obesity, graft-versus host disease and human immunodeficiency virus) [31] [32] [55].

1.3. The gastrointestinal tract in aging: Aging associated degradation and nitric oxide system in the GI tract

Aging associated degradation

The prevalence of GI diseases has been shown to rank high in the elderly population and to represent major sources of morbidity, mortality, and healthcare costs [15]. The most common disorders include oesophageal and swallowing difficulties, gastric and peptic ulcer disease, gastroparesis or delayed gastric emptying, irritable bowel syndrome, and inflammatory bowel disease [16]. Malnutrition is also a common problem in aged population, affecting the immune function, response to bacterial and viral infections, and loss of body weight and muscle mass, due to e.g., oral health problems, gastritis, decreased sensory function, reduced mobility etc. [17] [18].

Like any other organ and tissue, the intestinal barrier is affected by the ageing process. Studies in rodents and non-human primates reported that intestinal permeability increased with age and in some case, alteration of the expression of TJ components was observed [42] [43]. Likewise, aging has a negative impact on the intestinal barrier in humans, by inflicting damage to both TJ and AJ structures [98]. Furthermore, aging is associated with structural and functional mucosal defence defects, increased oxidative stress, diminished capacity to generate protective immunity, and increased incidence of inflammation and autoimmunity [35] [44].

Defective GI tract defence system and low-grade chronic inflammation, originating from the intestinal environment, have consequences beyond the gut, even affecting degenerative disorders of the central nervous system, such as Parkinson's [91] and Alzheimer's disease [33], multiple sclerosis [34] and depression [92] [45].

Experiments in Drosophila have shown an association between alterations of intestinal barrier integrity in the gut and age-associated metabolic and inflammatory patterns [93]. In rodents, the age-related intestinal barrier dysfunction has been associated with mucosal atrophy, impaired epithelium renewal and regeneration, and changed/decreased TJ structures [36] [37].

Studies in elderly patients with a focus on impaired intestinal epithelial barrier, its function and age-associated changes of the various components, are lacking [100]. However, some studies suggest that age-associated gut microbial dysbiosis increases intestinal permeability, leading to the leakage of microbial products into the circulation, therefore triggering systemic inflammation [97] and contributing to the aggravation of GI diseases [98]. The identification and clarification of the age-associated modifications of the various components of the impaired intestinal barrier, and the underlying mechanisms, is a much-needed step

required to design effective intervention strategies to address an array of late life-related disturbances that have a significant impact on health and well-being [41] [56].
Currently, there is no gold standard as sensitive, reproducible, and feasible method for measuring intestinal permeability in the clinical and preclinical setting [57]. Still there are highly reliable, diverse methods scientists rely on, depending on the experiments setting, the model species, the marker molecules, and the used compartments for measurement [101].

Nitric oxide system in the GI tract

Nitric oxide (NO) is responsible in multiple physiological functions of the GI tract, including: the maintenance of the mucosal integrity, gastric epithelium and vascular tone, the mediation of gastric blood flow, stimulation of mucus and bicarbonate secretion, resistance of epithelial cells to injury and downregulation of inflammatory mediator release [58]. NO is a free radical signalling molecule, which directly regulates the function of ion channels, enzymes, and a number of other proteins, and is generated through a series of regulated electron transfer steps by a family of P450-like enzymes, termed “NO synthases” (NOS) [59]. The oxidation of L-arginine to equimolar amounts of L-citrulline and NO is catalysed by one of three isoforms of NOS enzymes (Figure 4.). The endothelial NOS (eNOS) and neuronal NOS (nNOS) are expressed basally at the vascular endothelium and the enteric nervous system of the GI tract, and the inducible isoform (iNOS) is expressed in macrophages and neutrophils [60]. NO helps maintain homeostasis in the GI tract and, when disrupted, it can cause pathologic conditions [61].

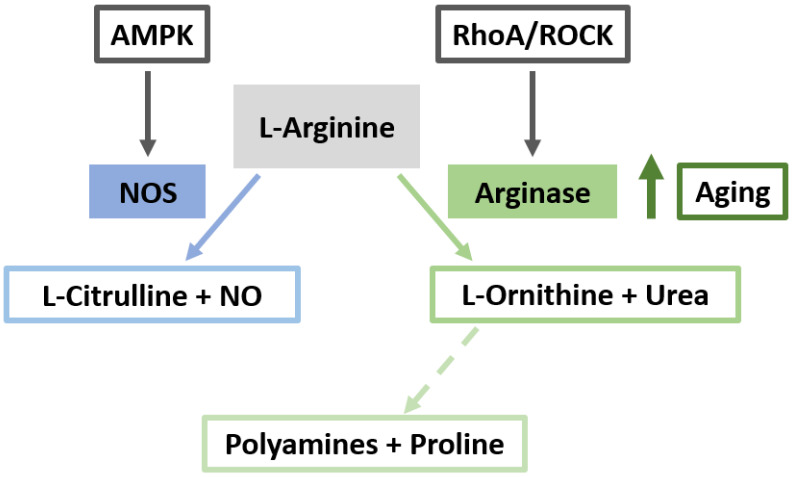

Figure 4: Schematic illustration of L-arginine pathways. Synthesis of L-citrulline and NO, or arginase catabolism to L-ornithine and urea, further production of polyamines and proline, and the involvement of AMPK and RhoA/ROCK. [71] [102]

Arginase is an enzyme from the ureohydrolase superfamily that catalyses the final step in the urea cycle converting L-arginine to L-ornithine and urea. It detoxicates from ammonia and produces ornithine for the polyamines and proline synthesis [62] (Figure 4.). In humans there are two isoforms of the enzyme, encoded by a separate gene, that produce the same metabolites and have similar mechanisms of action. Arginase 1, located in the cytosol, and arginase 2, located in the mitochondria, are almost identical in structure and the function's critical areas are homologous [63]. Pathological effects of overactive arginase, which can induce intestinal fibrosis, hypertrophy, neurodegeneration and tumorigenesis, show the importance of the balance between consumption of L-arginine by arginase and NOS [64]. In aging humans, as well in experimental animal models, the excessive arginase activity has been linked to the senescence of endothelial cells [65].

Unpublished data of the own working group show an increased intestinal arginase activity in aged rodents, alongside an intestinal barrier dysfunction. Besides, arginine supplementation improves intestinal barrier function [66], prevents bacterial translocation [67], activates the intestinal innate immunity [68], protects from radiation-induced inflammation [69] and enhances survival after intestinal mesenteric ischemia [70], in mice. On the other hand, data obtained from cell/animal models and small-scale clinical studies suggests that inhibiting arginase activity, by administration of arginase inhibitors, holds beneficial therapeutic potential for various pathological conditions [71] [72].

Increasing arginase expression and activity includes, inter alia, the activation of intracellular Rho kinase (ROCK) signalling cascade [78]. The importance of the Rho family, small guanosine triphosphate binding proteins, is present in the regulation of epithelial TJ function, structure and assembly [79]. Influencing the myosin phosphatase and myosin light chain, ROCK has a role of regulating the actin cytoskeletal contractility, therefore the TJ formation [80]. Y-27632, a ROCK inhibitor, enhances the paracellular permeability but does not influence the TJ proteins distribution, implying that it is due to actin cytoskeletal reorganization [81].

Adenosine monophosphate-activated protein kinase (AMPK) has an important role of a central metabolic and energy regulator, and is involved in the regulating of intestinal barrier function, gut epithelial differentiation and tight junction assembly [74]. Activation of the AMPK pathway increases the NOS expression [102]. L-arginine regulates rodents' small intestinal integrity, improves mucosal barrier functions and enhances the TJ proteins expression by activating the AMPK signalling pathway [73]. It is not yet fully understood the influence of AMPK onto the ras homolog gene family member A (RhoA) and Rho-associated protein kinase.

Restoring AMPK activity, changed by pathological conditions as inflammation, metabolic syndrome and aging, can therapeutically be used for treatment of various diseases [75]. 5-Aminoimidazole-4-carboxamide ribonucleoside (AICAR), a direct AMPK activator, accelerates assembly of intestinal TJ proteins independent of calcium availability [76] [77].

1.4. Objectives

Due to increase in the life expectancy, the proportion of elderly in the global population continues to rise [6]. However, while overall life expectancy is increasing, the 'healthy life span' is not increasing accordingly [82]. The role of changes in intestinal function and especially intestinal barrier function in old age has not been fully understood [100]. Studies suggests that changes of intestinal barrier function may not only be critical in the development of metabolic diseases but also aging associated decline and the so-called inflammatory damage [41] [56]. Here in, the interplay between the NOS and arginase pathways has received great interest in recent years [83] [84].

The aim of the present thesis was to determine how the arginase inhibitor nor-NOHA affects the intestinal permeability in aging mice. Specifically, the following questions were addressed:

1. Does the treatment with the arginase inhibitor nor-NOHA affect the expression of tight junction proteins in aged mice?
2. Are markers of senescence in the small intestine altered in aging?
3. Does modulating arginase activity trough nor-NOHA affect permeability in an ex vivo everted gut sac model using small intestinal tissue?
4. Does the alteration of the ROCK signalling cascade and AMPK-related signalling cascade affect permeability in an ex vivo everted sac model bult from small intestinal tissue?

2. Materials

2.1. RNA extraction, cDNA synthesis, real-time qPCR and primers

RNA extraction

Equipment

Stainless Steel Beads, 5 mm	QIAGEN, Hilden, Germany
TissueLyser II	QIAGEN, Hilden, Germany
Centrifuge Z216 MK	HERMLE Labortechnik GmbH, Wehingen, Germany
Mixing block	BOIER Technology, Hangzhou, China

Chemical reagents

TRIzol	Thermo Fisher Scientific, Waltham, USA
Chloroform ($CHCl_3$)	Carl Roth GmbH & Co. KG, Karlsruhe, Germany
100% Isopropanol ($CH_3CHOHCH_3$)	Carl Roth GmbH & Co. KG, Karlsruhe, Germany
75% Ethanol (C_2H_5OH)	Carl Roth GmbH & Co. KG, Karlsruhe, Germany
RNase-free water	Sigma-Aldrich Inc., Steinheim, Germany
Agarose	Carl Roth GmbH & Co KG, Karlsruhe, Germany
TRIS base ($C_4H_{11}NO_3$)	Carl Roth GmbH & Co KG, Karlsruhe, Germany
Boric acid (H_3BO_3)	Carl Roth GmbH & Co KG, Karlsruhe, Germany
Ethylenediaminetetraacetic acid (EDTA) ($C_{10}H_{16}N_2O_8$)	Carl Roth GmbH & Co KG, Karlsruhe, Germany

cDNA synthesis

Equipment

96-Well UV-Transparent Microplate	VWR International GmbH, Darmstadt, Germany
SpectraMax M3 Multi-Mode Microplate Reader	Molecular Devices, Biberach and der Riss, Germany
LifeECO Thermal Cycler	BIOER Technology, Hangzhou, China

Chemical reagents

RQ1 RNase-Free DNase	Promega Corporation, Wisconsin, USA
RQ1 RNase-Free DNase 10x Reaction Buffer	Promega Corporation, Wisconsin, USA
RQ1 DNase Stop Solution	Promega Corporation, Wisconsin, USA
Magnesium chloride 25mM ($MgCl_2$)	Promega Corporation, Wisconsin, USA
Reverse Transcription Buffer	Promega Corporation, Wisconsin, USA
dNTP mix (10mM)	Promega Corporation, Wisconsin, USA
RNasin® Ribonuclease Inhibitor	Promega Corporation, Wisconsin, USA
Random Primer	Promega Corporation, Wisconsin, USA
AMV reverse transcriptase (15U)	Promega Corporation, Wisconsin, USA
RNase-Free Water	Sigma-Aldrich Inc., Steinheim, Germany

Real-time qPCR

Equipment

RNase-free PCR tube strips and flat caps	BioRad Laboratories, München, Germany
96-Well Microplate	BioRad Laboratories, München, Germany
Cover foil	BioRad Laboratories, München, Germany
CFX Connect Real-Time PCR Detection System	BioRad Laboratories, München, Germany

Chemical reagents

RNase-Free Water	Sigma-Aldrich Inc., Steinheim, Germany
iTaq Universal SYBR Green Supermix	BioRad Laboratories, München, Germany
Primer (see 2.4)	

Software

CFX Manager Software	BioRad Laboratories, München, Germany

Primers

Table 1: Primer sequences used for the analysis of gene expression in real-time qPCR analysis

Gene	Primer sequences (5′–3′)
Ribosomal protein S18	F: GAAGATATGCTCATGTGGTGTTG
(18S rRNA)	R: CCATCCAATCGGTAGTAGCG
High mobility group box 1	F: CGCGCTGGCTGGAGAGTAAT
(HMGB1)	R: GAGGCACAGAGTCGCCCAGT
Occludin	F: CATCAGCCATGTCCGTGAGG
(Occ)	R: GGGGCGACGTCCATTTGTAG
Zonula occludens-1	F: GCAGACTTCTGGAGGTTTCG
(ZO-1)	R: CTTGCCAACTTTTCTCTGGC

F: Primer Forward; R: Primer Reverse

2.2. Everted gut sac model

Equipment

Thermostatic water bath	GFL, Gesellschaft für Labortechnik GmbH, Burgwedel, Germany
Oxymix (95% O_2 and 5% CO_2)	Air liquide, Schwechat, Austria
Petri dish	Laboratory equipment
Razor blade	Hugo Herkenrath GmbH & Co.KG, Sollingen, Germany
Ruler	Laboratory equipment
Scissors	Laboratory equipment
Gavage needle	Laboratory equipment
Syringe	Laboratory equipment
String	Laboratory equipment
Glass Pasteur pipettes	Laboratory equipment

Chemical reagents

Sodium chloride (NaCl)	Carl Roth GmbH & Co. KG, Karlsruhe, Germany
Potassium chloride (KCl)	Carl Roth GmbH & Co. KG, Karlsruhe, Germany

Magnesium sulphate anhydrous ($MgSO_4$)	Alfa Aesar, Thermo Fisher GmbH & Co, Kandel, Germany
Calcium chloride dehydrate ($CaCl_2 * H_2O$)	Carl Roth GmbH & Co. KG, Karlsruhe, Germany
HEPES ($C_8H_{18}N_2O_4S$)	Carl Roth GmbH & Co. KG, Karlsruhe, Germany
Potassium dihydrogen phosphate (KH_2PO_4)	Carl Roth GmbH & Co. KG, Karlsruhe, Germany
Bovine serum albumin (BSA)	Sigma-Aldrich Chemie GmbH, Steinheim, Germany
D-Xylose ($C_5H_{10}O_5$)	Merck Chemicals GmbH, Darmstadt, Germany
N-ω-Hydroxy-L-norarginine (nor-NOHA) ($C_5H_{12}N_4O_3$)	Bachem (UK) Ltd, St. Helens, United Kingdom
5-Aminoimidazole-4-carboxamide riboside (AICAR) ($C_9H_{14}N_4O_5$)	Sigma-Aldrich Chemie GmbH, Steinheim, Germany
ROCK inhibitor Y-27632 ($C_{14}H_{21}N_3$)	Sigma-Aldrich Chemie GmbH, Steinheim, Germany

2.3. D-Xylose assay

Equipment

Magnetic stirrer RSM-10HS	Phoenix Instrument GmbH, Garbsen, Germany
Stir bar	Carl Roth GmbH & Co KG, Karlsruhe, Germany
Mixing block	BIOER Technology, Hangzhou, China
96-well plate	VWR International GmbH, Darmstadt, Germany
SpectraMax M3 Multi-Mode Microplate Reader	Molecular Devices, Biberach and der Riss, Germany

Chemical reagents

Phloroglucinol ($C_6H_6O_3$)	Carl Roth GmbH & Co. KG, Karlsruhe, Germany
Glacial acetic acid (CH_3COOH)	Carl Roth GmbH & Co. KG, Karlsruhe, Germany

37% concentrated hydrochloric acid (HCl)	Carl Roth GmbH & Co. KG, Karlsruhe, Germany
D-Xylose ($C_5H_{10}O_5$)	Merck Chemicals GmbH, Darmstadt, Germany
Benzoic acid (C_6H_5COOH)	Carl Roth GmbH & Co. KG, Karlsruhe, Germany

Software

SoftMax Pro7 Software	Molecular Devices, Biberach an der Riss, Germany

2.4. Western blot: Total protein isolation, Bradford assay, SDS-polyacrylamide gel preparation, electrophoresis and antibodies

Total protein isolation

Equipment

Stainless Steel Beads, 5 mm	QIAGEN, Hilden, Germany
TissueLyser II	QIAGEN, Hilden, Germany
SONOREX DIGITEC DT 100 H Ultrasonic bath	Bandelin Electronic, Berlin, Germany
Centrifuge Z216 MK	HERMLE Labortechnik GmbH, Wehingen, Germany

Chemical reagents

RIPA buffer	Sigma-Aldrich Chemie GmbH, Steinheim, Germany
Protease inhibitor cocktail	Sigma-Aldrich Chemie GmbH, Steinheim, Germany
Phosphatase inhibitor cocktail 2	Sigma-Aldrich Chemie GmbH, Steinheim, Germany
Phosphatase inhibitor cocktail 3	Sigma-Aldrich Chemie GmbH, Steinheim, Germany

Bradford assay

Equipment

96-well plate	VWR International GmbH, Darmstadt, Germany
SpectraMax M3 Multi-Mode Microplate Reader	Molecular Devices, Biberach and der Riss, Germany

Chemical reagents

Bovine serum albumin (BSA)	Sigma-Aldrich Chemie GmbH, Steinheim, Germany
BioRad Protein Assay Dye Reagent Concentrate	BioRad Laboratories, München, Germany

SDS-polyacrylamide gel preparation

Equipment

Mini-PROTEAN Glass Plates	BioRad Laboratories, München, Germany
Mini-PROTEAN Short Plates	BioRad Laboratories, München, Germany
Mini-PROTEAN Spacer Plates (1,5 mm)	BioRad Laboratories, München, Germany
Mini-PROTEAN System Comb 15 well	BioRad Laboratories, München, Germany
Mini-PROTEAN Casting Stand Gaskets	BioRad Laboratories, München, Germany
Mini-PROTEAN Tetra Cell Casting Stands & Clamps	BioRad Laboratories, München, Germany
Mini-PROTEAN Gel Releasers	BioRad Laboratories, München, Germany

Chemical reagents

TRIS base ($C_4H_{11}NO_3$)	Carl Roth GmbH & Co KG, Karlsruhe, Germany
Acrylamide (C_3H_5NO)	Carl Roth GmbH & Co KG, Karlsruhe, Germany
Sodium dodecyl sulphate ($NaC_{12}H_{25}SO_4$) (SDS)	Carl Roth GmbH & Co KG, Karlsruhe, Germany
Ammonium persulfate ($(NH_4)_2S_2O_8$) (APS)	Carl Roth GmbH & Co KG, Karlsruhe, Germany
Tetramethylethylenediamine ($C_6H_{16}N_2$) (TEMED)	Carl Roth GmbH & Co KG, Karlsruhe, Germany

Electrophoresis

Equipment

Mixing Block MB-102	BIOER, Hangzhou, China
Centrifuge Z216MK	HERMLE Labortechnik GmbH, Wehingen, Germany
Mini-PROTEAN Tetra Vertical Electrophoresis Cell	BioRad Laboratories, München, Germany
PowerPac™ HC High-Current Power Supply	BioRad Laboratories, München, Germany

Chemical reagents

TRIS base ($C_4H_{11}NO_3$)	Carl Roth GmbH & Co KG, Karlsruhe, Germany
Sodium dodecyl sulphate ($NaC_{12}H_{25}SO_4$) (SDS)	Carl Roth GmbH & Co KG, Karlsruhe, Germany
Glycerol ($C_3H_8O_3$)	VWR International GmbH, Darmstadt, Germany
β-Mercaptoethanol (C_2H_6OS)	Carl Roth GmbH & Co KG, Karlsruhe, Germany
Bromophenol blue ($C_{19}H_{10}Br_4O_5S$)	Carl Roth GmbH & Co KG, Karlsruhe, Germany
Dithiothreitol ($C_4H_{10}O_2S_2$) (DTT)	Sigma-Aldrich Chemie GmbH, Steinheim, Germany
Precision Plus Protein Standard	BioRad Laboratories, München, Germany
Glycine ($C_2H_5NO_2$)	Carl Roth GmbH & Co KG, Karlsruhe, Germany

Western blot

Equipment

PVDF-Membrane Hybond P	BioRad Laboratories, München, Germany
Extra Thick Blot Paper	BioRad Laboratories, München, Germany
Orbi-Blotter TM	Benchmark, Frankfurt, Germany
Multifunction Rotor PS-M3D	Grant Instruments Ltd, Cambridge, England
Trans Blot Turbo Transfer System	BioRad Laboratories, München, Germany
Tubular cover film	ALLPAX GmbH & Co. KG, Papenburg, Germany
Impulse Table Welding Machine PM-FS-200-S	ALLPAX GmbH & Co. KG, Papenburg, Germany
ChemiDoc™ Imaging Systems XRS+	BioRad Laboratories, München, Germany

Chemical reagents

Glycine ($C_2H_5NO_2$)	Carl Roth GmbH & Co KG, Karlsruhe, Germany
TRIS base ($C_4H_{11}NO_3$)	Carl Roth GmbH & Co KG, Karlsruhe, Germany
Sodium dodecyl sulphate ($NaC_{12}H_{25}SO_4$) (SDS)	Carl Roth GmbH & Co KG, Karlsruhe, Germany
Methanol (CH_3OH)	Carl Roth GmbH & Co. KG, Karlsruhe, Germany
Ponceau S ($C_{22}H_{16}N_4O_{13}S_4$)	Carl Roth GmbH & Co KG, Karlsruhe, Germany
Albumin Fraction V	Carl Roth GmbH & Co KG, Karlsruhe, Germany
Nonfat dried milk powder	PanReac AppliChem ITW Reagents, Darmstadt, Germany
Tween® 20 ($C_{58}H_{114}O_{26}$)	Carl Roth GmbH & Co KG, Karlsruhe, Germany
SuperSignal™ West Dura Extended Duration Substrate	Thermo Fisher Scientific, Waltham, USA

Software

Image Lab Touch 2.4	BioRad Laboratories, München, Germany
Software Image Lab™ 6.0	BioRad Laboratories, München, Germany

Antibodies

Chemical reagents

B-Actin Antibody (C4): sc-47778	Santa Cruz Biotechnology, Dallas, USA
Occludin monoclonal antibody	Invitrogen, Thermo Fisher Scientific, Waltham, USA
Occludin (Phospho-Tyr287) Antibody #12934	Signalway antibody, Maryland, USA
MYLK Polyclonal Antibody #PA5-79716	Invitrogen, Thermo Fisher Scientific, Waltham, USA
Anti-mouse IgG, HRP-linked Antibody #7076	Cell Signaling Technology, Leiden, Netherland
Anti-rabbit IgG, HRP-linked Antibody #7074	Cell Signaling Technology, Leiden, Netherland

2.5. General consumables

Equipment	
Gloves	STARLAB GmbH, Hamburg, Germany
Lab pens	VWR Internatio nal GmbH, Darmstadt, Germany
Piston stroke pipette	Eppendorf AG, Hamburg, Germany
Serological pipette	Sarstedt AG & Co, Nürnbrecht, Germany
Multichannel pipette	Brand GmbH & Co KG, Wertheim, Germany
Pipette tip (10, 200, 1000 µL)	Sarstedt AG & Co, Nürnbrecht, Germany
Reaction container (0.5, 1.5, 2 mL)	Sarstedt AG & Co, Nürnbrecht, Germany
Falcon tubes (15, 50 mL)	Sarstedt AG & Co, Nürnbrecht, Germany
RNase-free microfuge tubes (1.5, 2 mL)	Thermo Fisher Scientific, Waltham, USA
Test Tube Racks	Carl Roth GmbH & Co KG, Karlsruhe, Germany
Vortex Reax 2000	Heidolph-Instruments, Schwabach, Germany
Scale	Sartorius AG, Göttingen, Germany
Weighing dishes	Carl Roth GmbH & Co KG, Karlsruhe, Germany
Foam cooler box	Laboratory equipment
Aluminium cooling block	Laboratory equipment
Cardboard Cryogenic Boxes and dividers	Laboratory equipment
Orion 420A pH meter	Orion Research, Inc., Jacksonville, USA
Forceps	Laboratory equipment
Stop watch	Carl Roth GmbH & Co KG, Karlsruhe, Germany
Beaker	Laboratory equipment
Nitrogen container	KGW-Isotherm Karlsruher Glastechnisches Werk-Schieder GmbH, Karlsruhe, Germany
Safety glasses	Laboratory equipment
Aluminium foil	Carl Roth GmbH & Co KG, Karlsruhe, Germany
Glass Erlenmeyer flask	Laboratory equipment
Glass Stopper	Laboratory equipment
Needle	Laboratory equipment
Floating Tube Racks	Laboratory equipment
Paraffin paper	Laboratory equipment
Plastic dish	Laboratory equipment

2.6. Software

GraphPad Prism 8.0	GraphPad Software Inc., La Jolla, USA
Microsoft Office 2019	Microsoft Corporation, Redmond, USA

3. Methods

3.1. Measurement of the gene expression

To determine the effects of aging on expression of markers of intestinal barrier, RNA was extracted from whole intestinal tissue, transcribed to cDNA, and analysed with qPCR. In the following, the steps of RNA isolation, cDNA synthesis and qPCR are summarised. To examine RNA transcripts, it is important to extract the RNA, with minimal degradation, from the tissues of interest [138]. First-strand cDNA is synthesized by the RNA-dependent DNA polymerase activity and should accurately represent the target DNA. Produced cDNA is used in the real-time quantitative polymerase chain reaction (qPCR) for analysing the gene expression [139].

3.1.1. Animal experiment

Tissue samples analysed in the present master thesis descend from animal experiment carried out previously by the research group of Prof. Dr. Ina Bergheim. Experiments were approved by the local institutional animal care and use committee and were carried out in accordance with the animal laws of Austria. Number: BMBWF-66.006/0014-V/3b/. In the following, procedures are described in brief. Male 3 months and 17 months old C57Bl/6 mice were housed in a SPF facility at the University of Vienna. Mice received a treatment with an arginase inhibitor N-ω-Hydroxy-L-norarginine (nor-NOHA) (10mg/kg BW, i.p.) or a vehicle (NaCl, i.p.) three times per week over six weeks. Standard chow and tap water were made available ad libitium at all times. The number of animals (n) was 6 to 8 per group. Before dissecting, the animals were intraperitoneally anaesthetised with ketamine and xylazine, the blood was collected, and they were killed by a cervical dislocation. Small intestinal tissue used in the present master thesis was snap frozen and stored at -80°C until further use.

3.1.2. RNA extraction

To obtain RNA a piece of frozen duodenal tissue was put in 1000 µL guanidinium thiocyanate (TRIzol), while handled on ice. The sample was homogenised by adding a 5mm stainless steel bead into the RNase-free microfuge tube and processing it in the TissueLyser mill, at the speed 25/sec, for 1 minute and then additional 30 seconds. Sample was mixed using a vortex mixer for 30 seconds and left at room temperature for 5 minutes to incubate. For the organic phase to be extracted and separated from the aqueous phase containing the RNA, 200 µL chloroform were added to each tube, put in the bead mill for 20 seconds, vortexed for 10 seconds, incubated 10 minutes at room temperature and finally centrifuged

for 10 minutes at 12000 rcf and at 4°C. The upper phase was transferred into a new tube, mixed with 500 µL isopropanol and incubated on ice for 15 minutes. The supernatant was carefully discarded, the remaining pellet was washed twice in 900 µL ethanol. The pellet was air dried for 10 minutes and solved in 40µl RNase free water on a block heater at 55°C for 10 minutes (300rpm). The samples were cooled on ice and stored at –80°C. RNA integrity was verified by agarose gel electrophoresis. Accordingly, 5 µL sample was mixed with 1 µL DNA dye on a piece of paraffin paper and transferred into the 1.5% agarose gel. 1x TRIS/Borate/EDTA (TBE) buffer was used (see Attachment) to make the agarose matrix. The electrophoresis was performed for 30 minutes at 110 V.

3.1.3. cDNA synthesis

To determine the RNA concentration spectrophotometric absorbance measurement was performed with a microplate reader, across three specific wavelengths. To indicate the presence of nucleic acids, since the absorption maximum of RNA lays at 260nm, samples were measured at 260nm. Some contaminants can be inferred from different wavelengths at which they are absorbed. For organic compounds, salts, urea, sugars it is 230nm and for protein at 280nm. Target ratios should comprise A260nm / A280nm ≈ 1.7 and A230nm / A260nm < 0.45 [140].

A 96-well UV-transparent microplate was used, containing 100 µL volume of diluted samples, in ratio 1:20 with aq. dest., and blanks, singly distilled water, in duplicates. RNA concentration was calculated as the multiplied values of the difference between absorption at 260nm and absorption of blank, the dilution factor and optical density unit. Based upon the nucleotide's extinction coefficient at 260nm in a light path of 1cm, a OD_{260} Unit equals the absorbance of 40µg/ml RNA [141].

$$c\,(RNA) = (A_{260}\text{-}A_{blank}) * \text{dilution factor (20)} * OD_{260}\ \text{Unit (40)}$$

Furthermore, samples were adjusted so that 8 µL distilled water contained 1.11 µg RNA.

To degrade single-stranded or double-stranded DNA, 1 µL RQ1 RNase-Free DNase and 1 µL of corresponding 10x reaction buffer were added to each tube and incubated in a thermocycler for 30 minutes at 37°C. The reaction was stopped with addition of 1 µL DNase Stop Solution, which developed for 10 minutes at 65°C. A master mix was created of all cDNA synthesis reaction components, shown in Table 2, and pipetted to the sample.

Table 2: Preparation of master mix for cDNA synthesis reaction

Substances	Mass
MgCl2 25mM	4 µL
Reverse Transcription Buffer	2 µL
dNTP mix 10mM	2 µL
RNAsin	0.5 µL
Random Primer	1 µL
AMV Reverse Transcriptase 15U	0.6 µL

The synthesis transacted in the thermocycler program at specific temperature and duration, shown in following table.

Table 3: Thermocycler program used for the cDNA synthesis

Duration	Temperature
10min	25°C
15min	42°C
5min	95°C
5min	4°C

Subsequently 80 µL RNase free water was added to each finished sample and stored at -20°C until following use.

3.1.4. Real-time qPCR

Amplifying the target DNA sequence and quantifying the concentration of that DNA species, was achieved by using the synthetized cDNA as a template for the quantitative real-time polymerase chain reaction. The method is considered the gold standard due to its sensitivity and accuracy [142]. In a two-step PCR the denaturation of the template DNA unwinds at the higher temperature. Followed by the second step consisting of the attaching of DNA primers to the template and enzymatic new strand production [143]. A DNA polymerase bonds to the primer and adds one by one the DNA bases to the single strand, in the 5' to 3' direction. For that purpose, a forward and reverse primer were chosen as starting points to fix at each end of the targeted DNA sequence [144]. Used iTaq Universal SYBR Green Supermix contains the thermostable iTaq DNA polymerase, it's cofactor $MgCl_2$, dNTPs mix of four basic nucleotides and a blend of reference dyes SYBR Green I [145]. To normalize the systematic variation and minimize sample-to-sample and quantification errors, the in-variant reference control (18S rRNA) was included as a housekeeping gene [146]. 5 µL of each cDNA sample was combined in a 96-well microplate with 15 µL of the following master mix, shown in Table 4.

Table 4: Preparation of master mix for quantitative real-time PCR

Substances	Mass
Primer Forward	1 µL
Primer Reverse	1 µL
RNase-free water	3 µL
iTaq Universal SYBR Green Supermix	10 µL

Samples were measured in duplicates and blanks were as well included. It was handled very precisely and clean while performed on ice. The upcoming Table 5 is displaying the specific genes and the corresponding duration and temperature profile as well as the number of cycle repetitions at which the gene expression was measured.

Table 5: Thermal cycling conditions for the quantitative real-time PCR protocols

Gene	Temperature	Duration in minutes	Repeated Cycles
18s rRNA	95 °C	0:30	/
	95 °C	0:05	25
	55 °C	0:30	
	95 °C	0:10	/
	65 °C	0:05	/
	95 °C	0:05	/
HMGB1	95 °C	0:30	/
	95 °C	0:05	44
	64 °C	0:30	
	95 °C	0:10	/
	65 °C	0:05	/
	95 °C	0:05	/
Occ, ZO-1	95 °C	0:30	/
	95 °C	0:05	49
	64 °C	0:30	
	95 °C	0:10	/
	65 °C	0:05	/
	95 °C	0:05	/

First 30 seconds / 95°C are prerequisite for the initial denaturation. The annealing and elongation temperatures, combined into one step, are compatible for each analysed gene and repeated as needed. Post-amplification steps are identical between the protocols, varying between 95, 65 and 95 °C, and the final analysis generating the melting curve.

3.2. The everted gut sac model

The so called ‘everted gut sac’ model is an ex-vivo model, developed and improved for more than six decades, for the investigation of intestinal enzymes and metabolic pathways, absorption mechanisms, membrane permeability and transporters [147]. In brief, to build the 'everted sac' from small intestinal tissue young and old male C57Bl/6 mice were housed in a SPF facility at the University of Vienna. The animals received standard chow, tap water ad libitium at all times and were killed by killed by cervical dislocation. First group (n=5) was 2 to 3 months old and their dissected intestine was incubated with the arginase inhibitor N-ω-Hydroxy-L-norarginine (nor-NOHA). In the next group of (n=7) male C57Bl/6 mice, three were 5 months old and the other four 22 to 23 months old. Their intestine was treated additionally with 5-aminoimidazole-4-carboxamide riboside (AICAR) and ROCK inhibitor Y-27632.

Procedure

Small intestinal tissue was removed incessantly and placed in a petri dish filled with ice cold KRH buffer (see Attachment). The tissue was cut in 3.5cm long tissue pieces. A gavage needle was put inside of the intestine and a small end part was left suspended, which got held with a second gavage needle. Carefully, without letting the tissue dry out, the intestine was slided on the other needle therewith turned inside out. The everted tissues end was gently pushed over the needles tip, held softly with dull forceps and a strong single knot was tied under the head of the gavage needle. The knot was repeated, placing it on top of the other. Using forceps, the intestine was gently slipped off and held at the tip of the gavage needle at which a syringe filled with buffer was placed. The intestine was filled with 100µL KRH buffer. While holding the open end of the intestine another knot was made under the needles head, forming a “sausage”. The length between the knots and weight before the incubation was measured and recorded [148f]. The ready everted gut sac models were randomly assigned to the incubation conditions. Stock solutions were made with the active substances and then diluted to the end volume of 5 mL KRH buffer and the needed end concentration, shown in Table 6.

Table 6: Preparation of the buffers and added compounds which the everted gut sac models were incubated in

Condition	Molarity (in 5mL KRH Buffer)
nor-NOHA 1	1 µM
nor-NOHA 10	10 µM
nor-NOHA 100	100 µM

Condition	Molarity (in 5mL KRH Buffer)
nor-NOHA	1 µM
AICAR 50	50 µM
AICAR 500	500 µM
ROCK 2	2 µM
ROCK 20	20 µM

Firstly, the everted gut sacs were incubated in an oxygenated (95% O_2 and 5% CO_2) falcon tube containing the different buffers compounds while heated in a water bath at 37 °C for 55 minutes. Additionally, they were transferred to the matching condition, which was made to the same volume and concentration as in Table 6, and in addition contained 0.1% (w/v) D-xylose, and incubated for extra 5 minutes, at 37 °C. After the incubation in D-xylose containing buffers, the inside content was collected and stored at –20 °C. Everted sacs weight was taken again. The knots were cut off and the remaining tissue placed in a reaction container, then frozen in liquid nitrogen and stored at -80°C.

3.3. D-Xylose assay to assess permeability

D-Xylose is a pentose, used to study intestinal function, that undergoes a non-enzymatic digestion and incomplete metabolization prior to absorption. Analysis of the monosaccharide uptake is a convenient and rapid investigative tool for researching the intestinal permeability markers in in-vitro settings [149]. To determine D-xylose permeation in the everted sac models a light sensitive acidic colour reagent was prepared in a glass Erlenmeyer flask, after the schema shown in Table 7. A stir bar was added, closed with a glass stopper, covered with aluminium foil and left to homogenise overnight at room temperature on a magnetic stirrer.

Table 7: Preparation of the reagent buffer for the measurement of D-xylose

Substances	Mass
Phloroglucinol	0.5 g
Glacial acetic acid	100 mL
37% conc. Hydrochloric acid	10 mL

To each reaction container 1000 µL of the colour reagent was pipetted under the fume hood. 10 µL of each corresponding D-xylose standard (see Attachment), standard blank (distilled water), sample (out of intestinal lumen) and sample blank (KRH buffer) was added. Measurements were performed in duplicates. Reaction tubes were vortexed and additionally a hole was made with a needle to each lid, to prevent uncontrolled thermal expansion. Samples were incubated in a heat block for 4 minutes at 100°C, and then transferred to a water bath to bring them at room temperature. 200 µL content of each container was transferred to a 96-well plate and measured in a spectrophotometer at 554nm.

The D-xylose concentration in the samples was calculated using standard curves. In order to convert from the measured concentration in mmol/L to µmol and further to µmol/cm, the weight of collected solution was calculated and the length of the intestine was incorporated. To minimize the variation between each analysed plate a tracking sample, taken from earlier studies. was measured with each one to serve the purpose of equalization.

3.4. Detection of protein levels in everted sac samples using Western blot

To determine the protein levels of β-actin, occludin, phospho-occludin and myosin light-chain kinase from snap-frozen intestinal tissue of everted sac experiments, the total protein was extracted with the RIPA buffer and its concentration measured with the Bradford protein assay. The proteins got separated by the gel electrophoresis and transferred onto a carrier membrane. Chemiluminescence detection of the target proteins took place with the binding of the primary and secondary antibodies onto them, and further visualization and analysis. In the following, the steps are described in detail.

Total protein isolation via RIPA

To the reaction container, containing the frozen tissue samples, a 5mm stainless steel bead and 100 µL of extraction solution (Table 8) were added. Samples were processed in the TissueLyser mill, at the speed 25/sec for 30 seconds, and in the ultrasonic bath, for 10 seconds. Furthermore, the samples were centrifuged for 15 minutes at 13200rpm and 4°C. 80 µL of the supernatant was transferred into a new tube and stored at –80°C.

Table 8: Preparation of the extraction solution for the total protein isolation

Substances	Mass
RIPA buffer (see Attachment)	1000 µL
Protease inhibitor I	100 µL
Phosphatase Inhibitor II	100 µL
Phosphatase Inhibitor III	100 µL

Bradford assay: Protein quantification

Using a BSA standard curve, made from the defined concentrations (shown in Table 11), the sample protein concentrations got calculated. To prepare the standard curve, the extraction buffer (RIPA) was diluted in the same ratio as the samples. The samples were diluted with aq. dest. in a ratio of 1:80. Samples, as well as the standards, were applied in triplicates. 5 µL of each was transferred into a 96-well microplate and 200 µL of colour reagent (dilution ratio 1:5, with aq. dest.) was added. The plate was shaken for 5 minutes in the microplate reader prior the measurement at A_{590} nm.

Table 9: Standard serial dilution used for the protein quantification in the Bradford assay

	Protein	***Extraction buffer***	***Concentration [mg BSA/mL]***
A	2 µL BSA stock solution	198 µL	1.0
B	100 µL A	100 µL	0.5
C	100 µL B	100 µL	0.25
D	100 µL C	100 µL	0.125
E	100 µL D	100 µL	0.0625
F	/	100 µL	0

SDS-polyacrylamide gel preparation

For the protein separation, according to their molecular mass, 10% separating and 5% stacking SDS-polyacrylamide gels were prepared. The composition is shown in Table 9 and Table 10. Preparation of the used solutions is shown in the attachment.

Table 10: Composition of the 10% separating SDS-polyacrylamide gel

for 2 gels at 1 mm spacer

Substances	**Mass**
Aq. dest.	4170 µL
1,5 M TRIS (pH 8,8)	2600 µL
30 % Acrylamide	3300 µL
10 % SDS	100 µL
10 % APS	100 µL
TEMED	6 µL

Table 11: Composition of the 5% stacking SDS-polyacrylamide gel

for 2 gels at 1 mm spacer

Substances	**Mass**
Aq. dest.	1512.5 µL
0.5 M TRIS (pH 8,8)	625 µL
30 % Acrylamide	312.5 µL
10 % SDS	25 µL
10 % APS	25 µL
TEMED	3 µL

Electrophoresis

After the protein concentration was determined using the Bradford assay, the amount of protein required for each sample, to load the gel for the electrophoresis, was calculated. Samples were set to the target concentration of 3 µg/µL and 1 µg/µL. Membranes loaded with 1 µg/µL protein were used for the detection of β-actin and phospho-occludin, and the membranes with the 3 µg/µL protein concentration for occludin and myosin light-chain kinase (MYLK). The stated concentrations of each sample were brought to the equal volume of 15 µL by adding the applied extraction solution and 3.75 µL SDS loading buffer (see Attachment). After the sample-buffer mixture was prepared, 2.25 µL dithiothreitol (DTT) was added, to complete the denaturation of protein, and then treated for 5 minutes on 95°C, using a mixing block. The samples were cooled down by shortly centrifuging them at 4°C. Finally, 2 µL of the protein standard (ladder) and 10 µL of samples were applied to the built-in gel, and separated in the gel electrophoresis chamber at 110V for 1.5 hours. The electrophoresis buffer (see Attachment) was diluted 1:10 before the usage.

Semi-dry blotting

The separation of the proteins was followed by the transfer of the samples to a polyvinylidene fluoride (PVDF) membrane. First, the PVDF membrane was activated with methanol for 10 seconds, and then placed in transfer buffer (see Attachment) together with two filter papers, to shake on low speed, for 10 minutes. The loaded gels were also placed in transfer buffer for 10 min and shaken for equilibration. The gel and membrane were finally placed between the filter papers (Figure 5.) and the protein transfer took place in the turbo blotter (25V, 1A) for 30 minutes. The loaded membrane was dried overnight in order to be able to continue with the further membrane treatments.

Figure 5: Structure of the "blotting sandwich"

Ponceau S staining

To locate the position of the transferred proteins and verify the equal loading of samples, Ponceau S staining was performed [113]. The dried membrane was activated again with methanol for 20 seconds, then shaken in aq. des. for 10 seconds and transferred into Ponceau S (see Attachment) for 3 minutes, further shaken at low speed. After the Ponceau-stained membrane was controlled for a uniformed protein separation, it was washed in aq. des. three times, for 20 seconds each.

Antibody incubation and protein detection

To avoid non-specific binding of undesired proteins, the membrane was blocked for 1 hour on a microplate shaker at room temperature, by incubating it: for β-Actin and MYLK in a solution of 2,5% BSA dissolved in 1xTBST, and for occludin and phospho-occludin 5% MMP in 1xTBST (see Attachment). The primary antibody incubation (see Table 12) occurred at room temperature on a rotating table for 2 hours for β-Actin membranes. The occludin, phospho-occludin and MYLK incubation was at 4°C on a rotating table, overnight. After the primary incubation the membrane was washed three times for 10 minutes in 1xTBST. The secondary antibody incubation took place at room temperature for 75 minutes on a shaker at low speed. Anti-mouse IgG was used for β-actin and occludin, and anti-rabbit IgG for phospho-occludin and MYLK. Again, the membrane was washed three times for 10 minutes in 1xTBST.

Table 12: Used dilutions for the antibody incubation

Protein	Dilution
β-Actin	P: 1:500 (2,5% BSA in 1xTBST)
(ACTB)	S: 1:5000 (2,5% BSA in 1xTBST)
Occludin	P: 1:500 (5% MMP in 1xTBST)
(Occ)	S: 1:5000 (5% MMP in 1xTBST)
Phospho-occludin	P: 1:500 (5% MMP in 1xTBST)
(pOcc)	S: 1:5000 (5% MMP in 1xTBST)
Myosin light-chain kinase	P: 1:2000 (2,5% BSA in 1xTBST)
(MYLK)	S: 1:5000 (2,5% BSA in 1xTBST)

P: Primary antibody; S: Secondary antibody

The last step was the detection of the bands. For this purpose, the membrane was placed in a plastic dish with a 1: 1 diluted solution of peroxidase buffer and luminol for 5 minutes and afterwards transferred into the imager. The densitometric evaluation of the bands was carried out with the help of the Image Lab ™ 6.0 software. The volume intensity of occludin was normalised with the β-actin.

3.5. Data analysis

The statistical evaluation and graphical representation of all data were performed with the software GraphPad Prism 8.0. Statistical differences were determined using Mann-Whitney test for comparing two groups or a two-way ANOVA test. For analysing data of everted gut sac one-way ANOVA was used. Statistical outliers were checked using Grubb's test. All data are presented as mean values (MW) ± standard error (SEM = standard error of mean).

4. Results

4.1. Expression of tight junction proteins in small intestinal tissue of young and old mice treated with the arginase inhibitor nor-NOHA

To determine if the arginase inhibitor nor-NOHA affects markers of intestinal barrier function in young and old mice mRNA expression of occludin as well as zonula-occludens-1 in proximal small intestine, of young (3 monhts old) and old (17 monhts old) animals treated for 6 weeks / 3 times weekly with either nor-NOHA or vehicle (sodium chloride), was analysed.

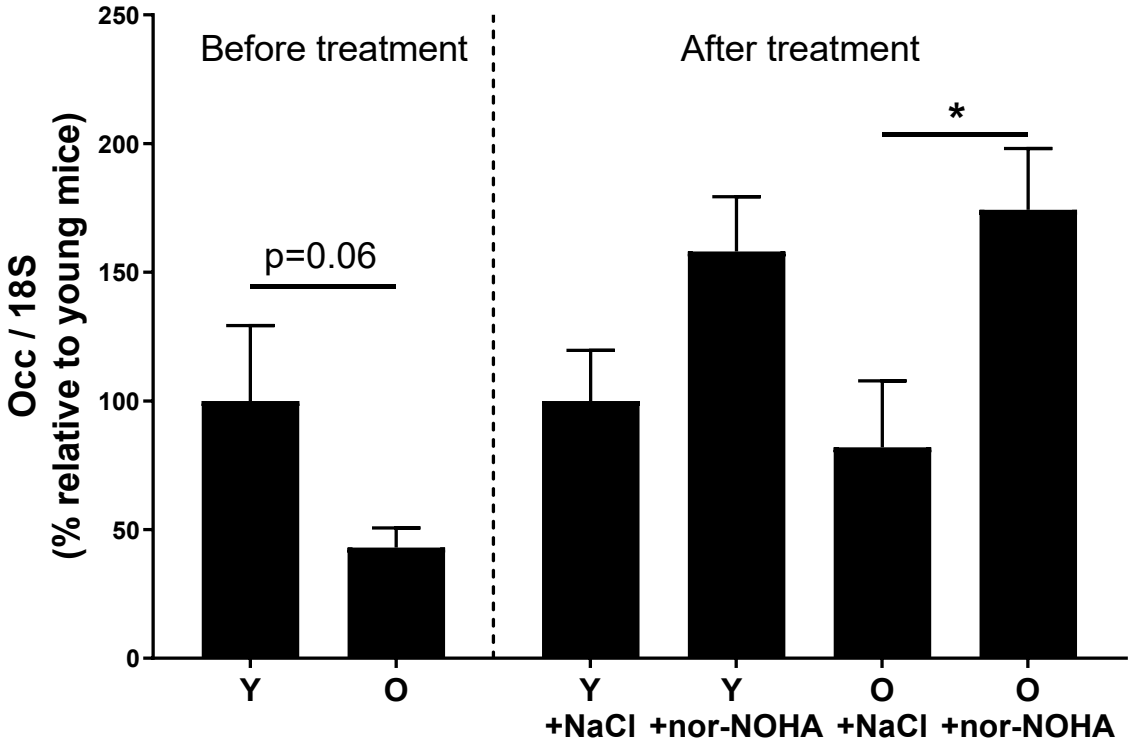

Figure 6: Expression of occludin (Occ) mRNA in proximal small intestine tissue of young (3mo) and old (17mo) mice before and after the treatment with the arginase-inhibitor N-ω-Hydroxy-L-norarginine (nor-NOHA) or vehicle (NaCl). *Mice were treated for 6 weeks 3 times weekly with either nor-NOHA or vehicle. n=6-8 mice/group. Results are given as percentage relative to young mice. Data presented as means +/- SEM. * p ≤ 0.05.*

Before the treatment expression of occludin mRNA in small intestinal tissue was by tract lower in old mice then in young (p=0.06). In young mice, the treatment with nor-NOHA had no effect on occludin mRNA expression, while in old mice the treatment with nor-NOHA was associated with significantly higher occludin mRNA in small intestinal tissue compared to vehicle treated mice (p≤0.05).

Furthermore, mRNA expression of occludin in small intestinal tissue of the vehicle treated young and old mice was similar while being lower than in young and old mice treated with nor-NOHA.

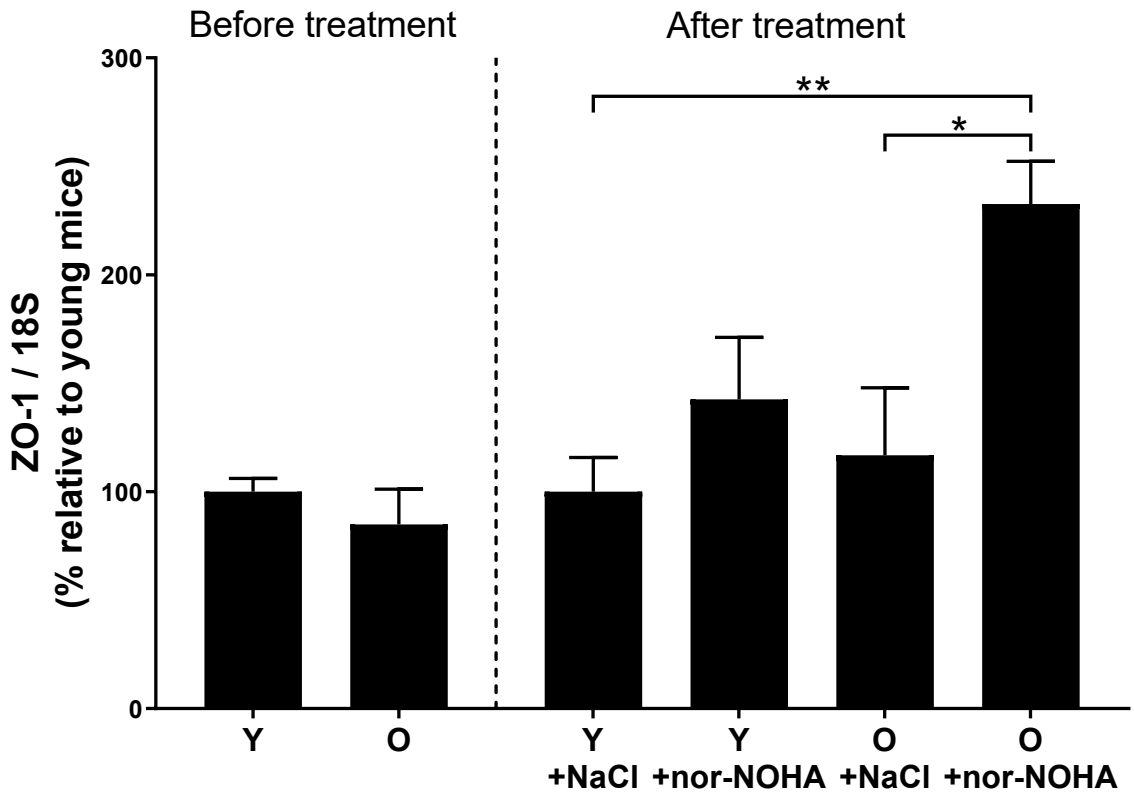

Figure 7: Expression of zonula occludens-1 (ZO-1) mRNA in proximal small intestine tissue of young (3mo) and old (17mo) mice before and after the treatment with the arginase-inhibitor N-ω-Hydroxy-L-norarginine (nor-NOHA) or vehicle (NaCl). *Mice were treated for 6 weeks 3 times weekly with either nor-NOHA or vehicle. n=6-8 mice/group. Results are given as percentage relative to young mice. Data presented as means +/- SEM. * p ≤ 0.05. ** p ≤ 0.01.*

While there was no significant difference for mRNA expression of ZO-1 between young and old mice before the intervention, treatment with the inhibitor nor-NOHA was associated with a significant upregulation of the ZO-1 mRNA expression in old mice compared to vehicle treated old mice ($p \leq 0.05$). Furthermore, the mRNA expression of ZO-1 in old nor-NOHA treated mice was also significaly higher than in young vehicle treated mice ($p \leq 0.01$).

4.2. Expression of senescence marker in small intestinal tissue of young and old mice treated with an arginase inhibitor nor-NOHA

To determine if the arginase inhibitor nor-NOHA affects senescence marker in proximal small intestine tissue of young and old mice, mRNA expression of HMGB1 was measured. In an intervention mouse experiment, young (3 monhts old) and old (17 monhts old) animals were treated for 6 weeks, 3 times weekly, with the inhibitor or vehicle (sodium chloride).

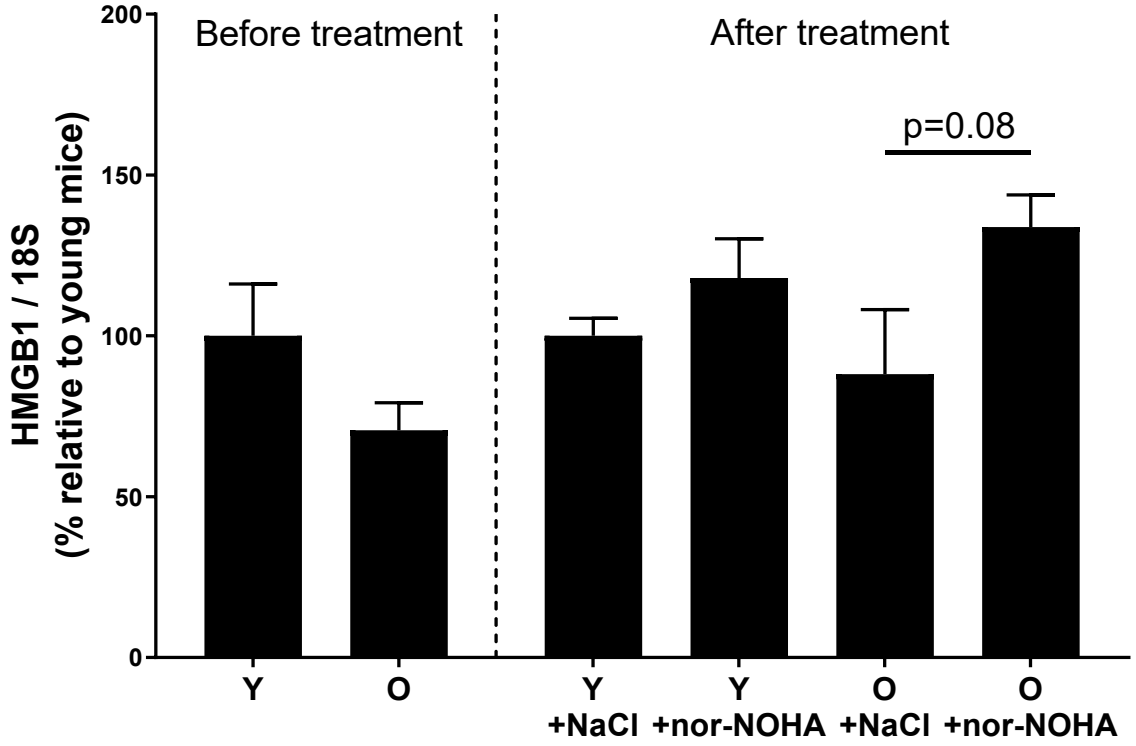

Figure 8: Expression of high mobility group box-1 protein (HMGB1) mRNA in proximal small intestine tissue of young (3mo) and old (17mo) mice before and after the treatment with the arginase-inhibitor N-ω-Hydroxy-L-norarginine (nor-NOHA) or vehicle (NaCl). *Mice were treated for 6 weeks 3 times weekly with either nor-NOHA or vehicle. n=6-8 mice/group. Results are given as percentage relative to young mice. Data presented as means +/- SEM.*

Before the treatment, the old group of animals showed lower mRNA expression of HMGB1 in small intestinal tissue compared to the young group. Treatment with the inhibitor nor-NOHA was associated with higher HMGB1 mRNA expression in old mice compared to vehicle treated old mice (p=0.08).

4.3. Effects of nor-NOHA on intestinal permeability in everted small intestinal tissue sacs of young mice

To determine if nor-NOHA affects intestinal permeability, everted sacs of small intestinal tissue of young mice were incubated with different concentrations of the arginase inhibitor.

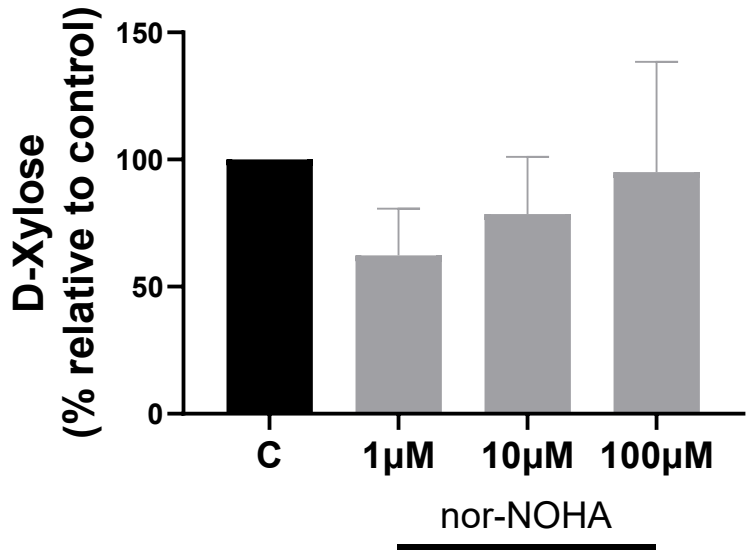

Figure 9: Effect of N-ω-Hydroxy-L-norarginine (nor-NOHA) on permeation of D-xylose in everted sacs bult from small intestinal tissue of young mice (2-3mo). *n=3-4 mice/group. Results are given as percentage relative to control. Data presented as means +/- SEM.*

Applied concentrations of nor-NOHA reduced the intestinal permeability of D-xylose, however not significantly. For the following experiment, the lowest substance amount (1µM) was applied thus it showed the greatest effect.

4.4. Effects of nor-NOHA, AICAR and Y-27632 on intestinal permeability and arginase activity in everted small intestinal tissue sacs of young and old mice

To determine if an inhibition of arginase, an adenosine monophosphate protein kinase activation and a rho-associated protein kinase inhibition affect the intestinal permeability, everted sacs of small intestinal tissue of young and old mice were incubated with nor-NOHA and different concentrations of AICAR and Y-27632.

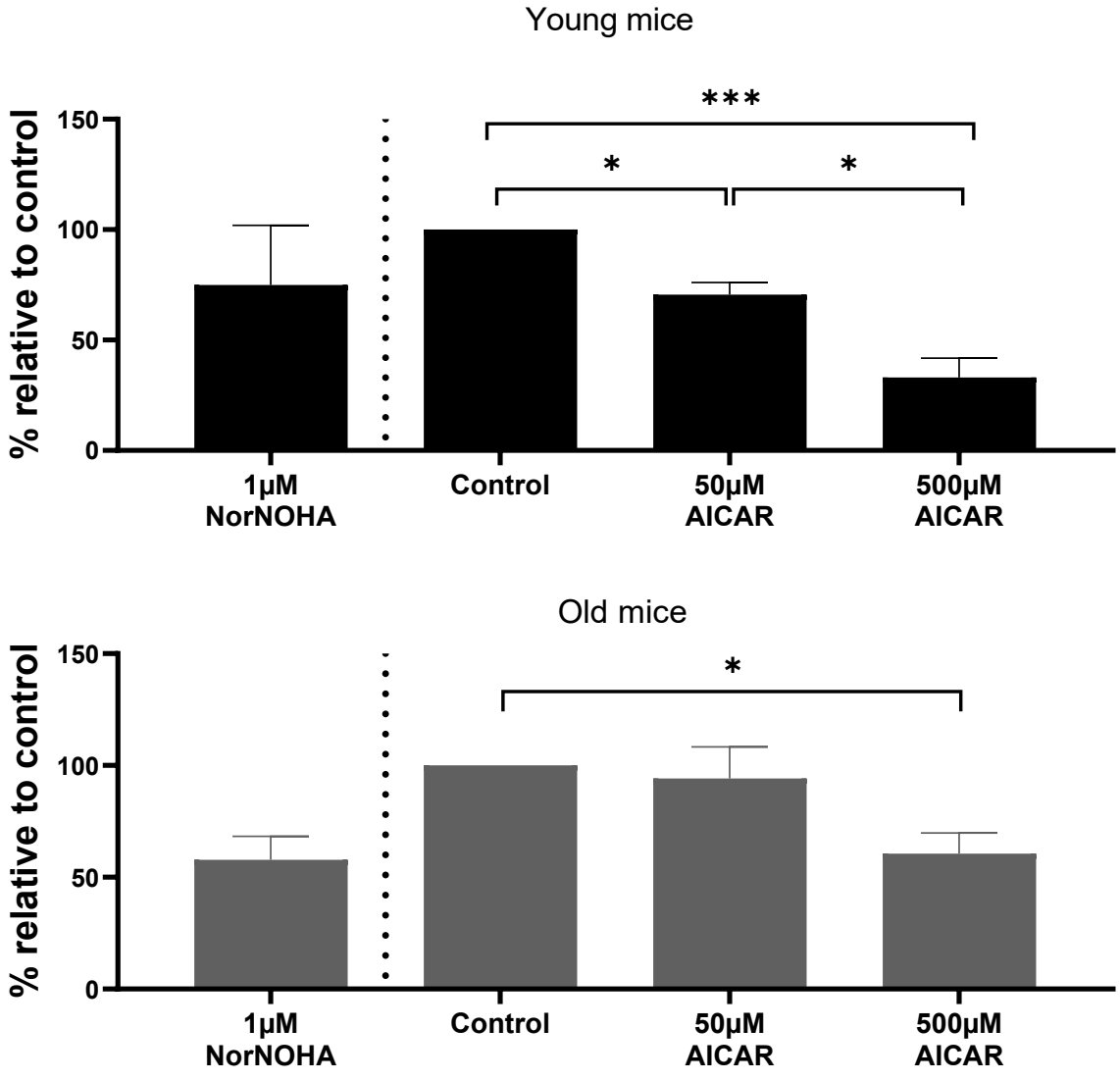

Figure 10: Effect of N-ω-Hydroxy-L-norarginine (nor-NOHA) and 5-aminoimidazole-4-carboxamide riboside (AICAR) on permeation in everted sacs bult from small intestinal tissue of young (5mo) and old (22-23mo) mice. *n=3-4 mice/group. Results are given as percentage relative to control. Data presented as means +/- SEM. * p ≤ 0.05. *** p ≤ 0.001.*

In everted sacs of intestinal tissue of young mice, the highest concentration of AICAR (500µM) reduced the D-xylose permeation very significantly (p≤0.001) compared to the control and significantly (p≤0.05) compared with the lower concentration of the AMPK activator (50µM). Additionally, 50µM AICAR decreased the permeation significantly (p≤0.05) in relation to the control. Furthermore, D-xylose permeation in the everted small intestinal tissue sacs of old mice was significantly (p≤0.05) lowered by the treatment with the higher AICAR concentration (500µM) relative to control.

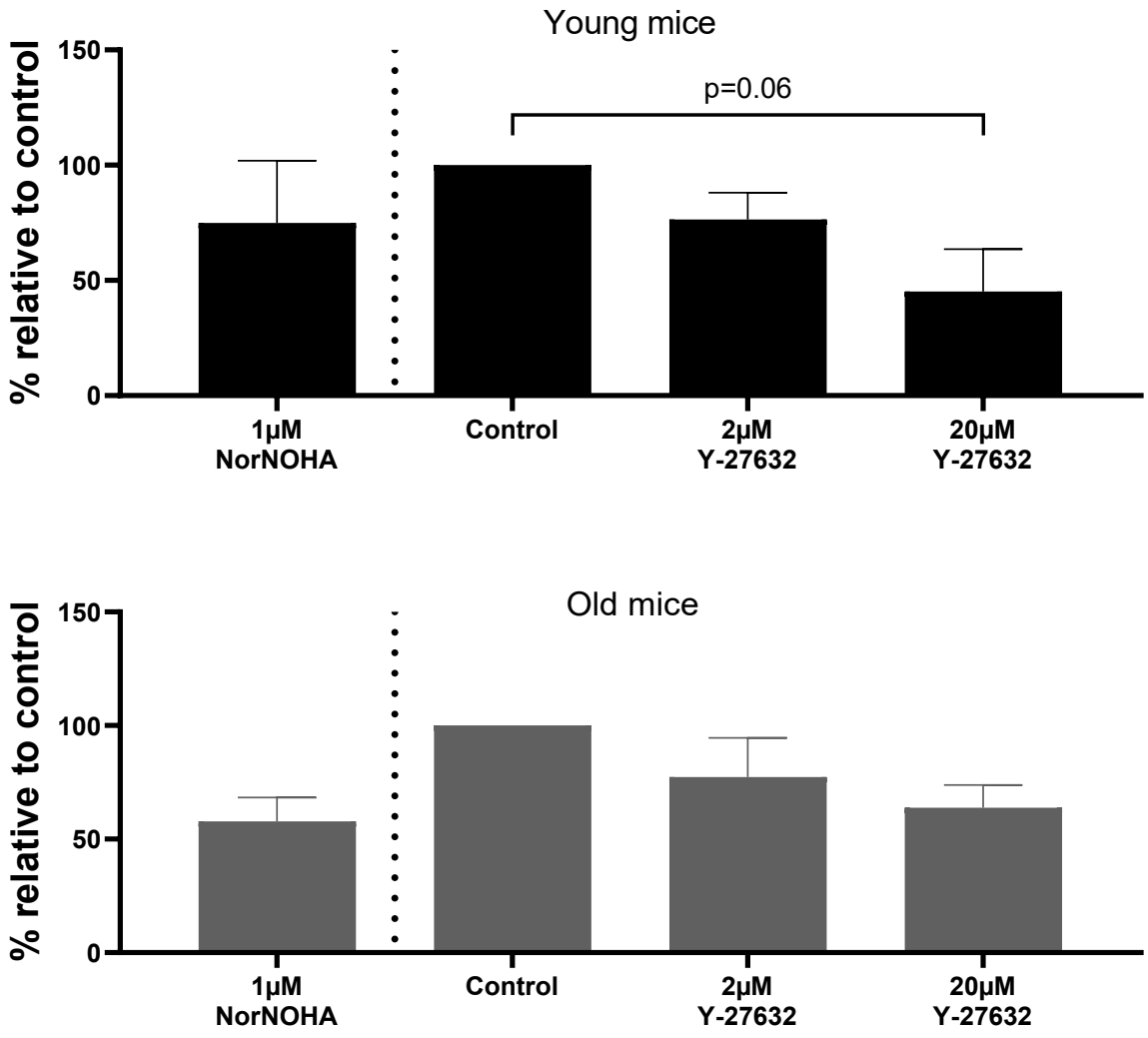

Figure 11: Effect of N-ω-Hydroxy-L-norarginine (nor-NOHA) and ROCK inhibitor (Y-27632) on permeation in everted sacs bult from small intestinal tissue of young (5mo) and old (22-23mo) mice. *n=3-4 mice/group. Results are given as percentage relative to control. Data presented as means +/- SEM.*

In small intestinal everted sacs build from tissue of young mice, the incubation with 20µM ROCK inhibitor Y-27632 reduced the D-xylose permeability compared to control (p=0.06). Both applied concentrations of Y-27632 decreased the intestinal permeability of D-xylose in everted sacs of intestinal tissue of old mice, however not significantly.

4.5. Effects of nor-NOHA, AICAR and Y-27632 on protein detection in everted small intestinal tissue sacs of young and old mice

Due to a lack of suitable samples for Western blot analysis, in the following only representative pictures of Western blot of everted small intestinal tissue sacs of young mice treated with of N-ω-Hydroxy-L-norarginine are shown.

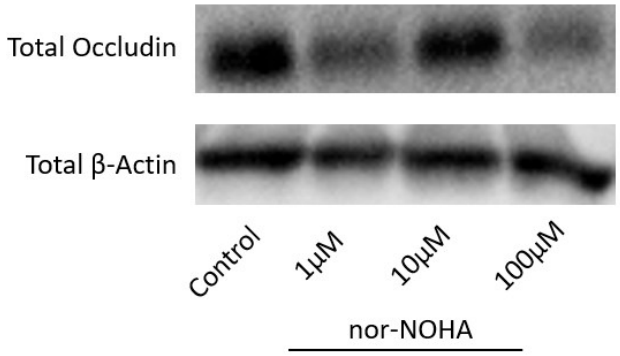

Figure 12: Representative Western blot of occludin and β-actin, from everted sacs bult from small intestinal tissue of young mice (2-3mo) treated with N-ω-Hydroxy-L-norarginine (nor-NOHA).

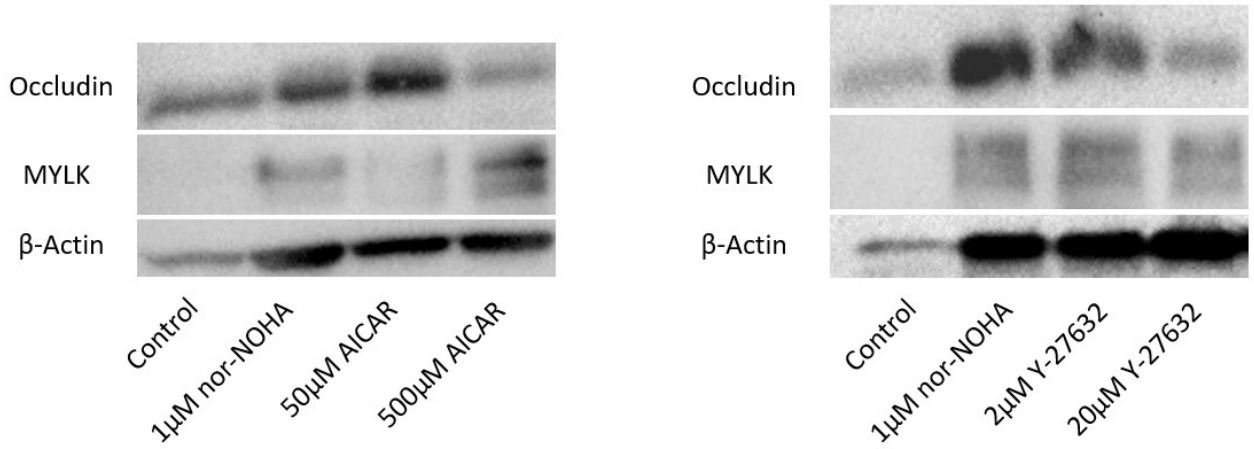

Figure 13: Representative Western blot of occludin, myosin light-chain kinase, and β-actin, from everted sacs bult from small intestinal tissue of young mice (5mo) treated with N-ω-Hydroxy-L-norarginine (nor-NOHA), 5-aminoimidazole-4-carbox-amide riboside (AICAR) and ROCK inhibitor (Y-27632).

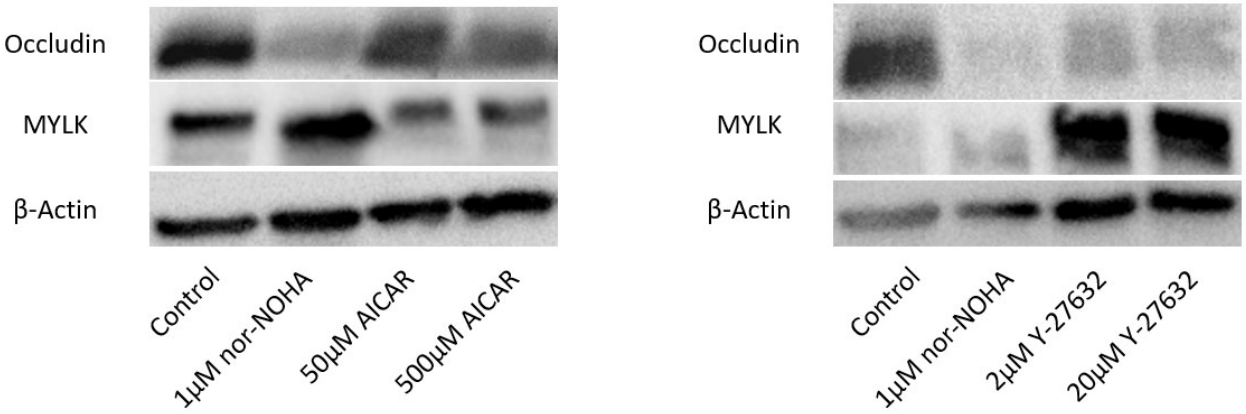

Figure 14: Representative Western blot of occludin, myosin light-chain kinase, and β-actin, from everted sacs bult from small intestinal tissue of old mice (22-23mo) treated with N-ω-Hydroxy-L-norarginine (nor-NOHA), 5-aminoimidazole-4-carbox-amide riboside (AICAR) and ROCK inhibitor (Y-27632).

Result of the measurements were quite vaguely, therefore no particular conclusion could be driven from them. To further clarify, samples were detected for the phosphorylation of occludin on tyrosine (Tyr), for its regulatory role in tight junctions [133].

4.6. Effects of nor-NOHA and Y-27632 on phospho-occludin protein concentration in everted small intestinal tissue sac of old mice

To determine if the inhibition of arginase or the rho-dependent signalling affects the concentration of tight junction proteins like occludin or phosphorylated occludin in everted sacs of small intestinal tissue of old mice, Western blot was performed and analysed. The phosphorylated version of the tight junction protein was compared to the primary occludin. Small intestinal everted tissue sacs of old mice were incubated with the higher concentration (20µM) of ROCK inhibitor, due to the results of D-xylose permeation.

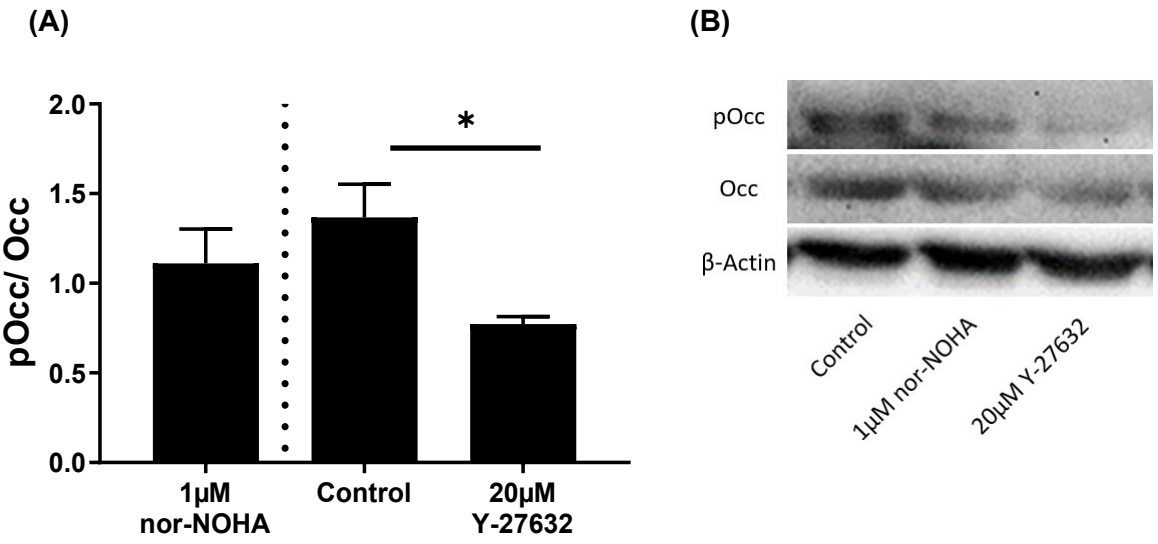

Figure 15: (A) Protein concentration of phospho-occludin (pOcc) relative to occludin (Occ) in small intestinal tissue of aged mice (22-23mo) treated with N-ω-Hydroxy-L-norarginine (nor-NOHA) and ROCK inhibitor (Y-27632). (B) Representative Western blot. *n=3-4 mice/group. Data presented as means +/- SEM. Arrangement of conditions differs between (A) and (B).*

As summarised in the figure 15 (A) the ratio of phospho-occludin to total occludin was significantly lower in everted sacs incubated with Y-27632 compared to vehicle treated sacs ($p \leq 0.05$).

5. Discussion

Because age-dependent alterations in GI barrier permeability are demonstrated both in animal and human studies [129] and growing body of evidence exists of arginase involvement in the aging process [130] [84], the main research question of the present thesis was to determine if and how the arginase inhibitor nor-NOHA affects the permeability in small intestinal tissue of aging mice and its influence on tight junction protein expression. Furthermore, the question whether this is related to alterations in AMPK and ROCK signalling, was addressed by an ex vivo model of small intestinal tissue e.g., an everted gut sac model.

Human studies have shown that an age-dependent increase in permeability of the GI barrier plays a role in the decreased barrier function and further pathogenesis [124]. Specifically, in epithelial cells, tight junction complexes are major regulators of cell-cell interactions [53]. Studies in rodents suggest that age-related changes in intestinal structure, such as increased endothelial gaps, are in part culpable for the decreased barrier function and increased permeability [125]. Furthermore, a study has shown that the mRNA expression of occludin and ZO-1 in intestinal epithelial cells is down-regulated with aging [36]; significant differences were shown between young (3 months), adult (12 months) and old (24 months) rats, associating the age-dependent discontinuous TJ structures to intestinal barrier dysfunction. In aging humans the TJ protein expression and formation tend to diminish as well, affecting the decline of barrier integrity [137]. In line with the data, the present study shows the mRNA expression of tight junction protein occludin in untreated small intestinal tissue of old mice is by tract lower than in young mice.

Numerous signalling molecules are linked to the tight junctions e.g., kinases and phosphatases interact with the proteins, indicating that the TJs are dynamically regulated by intracellular signal transduction [126]. Changes in tyrosine phosphorylation of ZO-1 and disturbance of the TJ barrier have been associated [128]. The significance of tyrosine phosphorylation status of ZO-1 in everted intestinal sacs of rodents was presented in the study from Hamada et al. (2010). No differences were shown in ZO-1 mRNA or protein expression levels in small intestinal tissue of rats between control and the treated group, however the examination of variation in ZO-1 tyrosine phosphorylation in rat intestine revealed a significant level difference [127]. In the present study, probably due to the large variation within groups, mRNA expression of ZO-1 in small intestinal tissue was not different between aged groups. Suggesting for further studies to incorporate an immunoprecipitation analysis to take into consideration the ZO-1 phosphorylation level.

The role of arginine, its metabolites and the nitric oxide synthesis pathway in the maintenance of gut function has been discussed more than two decades ago and is still an important field of research [120]. In previous studies performed by the own research group, unpublished data have shown that intestinal arginase levels are elevated with aging mice.
The arginase inhibitor nor-NOHA induces significantly higher mRNA expression of occludin and zonula-occludens-1 in small intestinal tissue of old mice. Furthermore, nor-NOHA treatment markable increased the ZO-1 mRNA expression in old mice in comparison to young vehicle treated mice. Results indicate that tight junction proteins occludin and ZO-1, contributing to the intestinal barrier strength [114], are upregulated with the arginase inhibitor treatment. The data contributes clearer understanding of the nitric oxide impact on the intestinal barrier structure, functions, and associated mechanisms of action [115] [116].
Besides the positive effect of arginase inhibitor on the GI barrier, it's impact on the senescence marker (high mobility group box-1 protein) in proximal small intestine tissue was determined. The treatment of mice with nor-NOHA was associated with higher HMGB1 mRNA expression in old mice, as to vehicle treated old mice. Mouse cell models in culture and in vivo support the claim that the increase of senescent cells with age and the response to senescence causing stimuli is featured with the depletion of nuclear HMGB1 (high mobility group box-1), it's relocation to the extracellular space from the nucleus [10] [11].
Inhibition of arginase with nor-NOHA reduced the intestinal permeability of D-xylose in everted sacs of small intestinal tissue of young and old mice, however not significantly.
Studies in rodents suggest that AMP-activated protein kinase might be critical in the regulation of arginase activity in the gut. AMPK has been suggested to have a critical role in the intestinal barrier function [122] and the AMPK activation may promote the formation and assembly of epithelial tight and adherens junctions [121]. In addition, a study demonstrated that the inhibition of AMPK attenuated the barrier dysfunction [131]. In the present study treatment of everted small intestinal tissue sacs with KRH buffer and AICAR, a direct AMPK activator, reduced the permeation very significantly in the group of young mice compared to the control, and significantly compared with the lower concentration of the AMPK activator. Furthermore, the permeability was significantly lowered by AICAR in sacs of old mice relative to controls. Which underlines the role of AMPK in age-associated disorders of the intestinal barrier.
Rho kinase (ROCK) signalling cascade includes arginase expression and activity [78], therefore the present thesis analysed the importance in the regulation of GI barrier function and permeability. ROCK has an influence on epithelial TJ function, structure and assembly [79] and regulates the TJ formation [80].

Y-27632 reduced the small intestinal permeability, compared to control, in everted sacs of young mice. This analysis supports the theory that ROCK inhibition decreases cellular permeability and stabilizes TJ proteins [123].

The phosphorylation of occludin has an important role in the maintenance and assembly of the TJ structures [133]. Occludin is highly phosphorylated on the serine and threonine residues in the intact epithelium, whereas tyrosine phosphorylation is undetectable [132]. Studies show that tyrosine phosphorylation of occludin is caused during disassembly by numerous stimuli [126]. Underlying this mechanism, Tyr phosphorylation attenuates the occludin interaction with ZO-1 and ZO-3, causing loss of binding and dissociation from the junctional complex [134] [135]. The inhibition of rho-dependent signalling in everted sacs of small intestinal tissue of old mice significantly reduced the ratio of phosphorylated to primary occludin, compared to vehicle treated sacs. Results suggest the ROCK inhibition attenuates the disruption of TJs, leading to a more intact GI barrier [136].

Further implications for upcoming practices are to approach the question of intestinal permeability with numerous differing techniques and methods. It is recommended to find a suitable indicator for a healthy aging process; thus, hallmarks of senescent cells are antagonistic and damage responsive [118]. Statistical uncertainty of this data is impacted by the small sample size and inconstant age of rodents. Furthermore, the generalizability of the results is limited by the species, type and gender of the experimental animal model [119]. Due to the lack of lengthy trials, the results cannot scope any follow up treatment.

6. Conclusion

This study aimed to determine if a dysfunction of NO metabolism is critical in aging associated decline of intestinal barrier dysfunction. Based on the expression of markers of intestinal barrier function, it can be concluded that nor-NOHA significantly upregulates tight junction protein mRNA expression, therefore strengthening the intestinal barrier [114]. The arginase inhibitor nor-NOHA has an important impact on the senescence marker (HMGB1) too. It is associated with a higher HMGB1 expression, indicating the decrease of senescent cells with age [10]. The results indicate that a direct AMPK activator (AICAR) very significantly reduces the permeation in everted small intestinal tissue sacs of young and old mice, emphasizing the role of AMPK-related signalling cascade in age-related disorders of the intestinal barrier. Additionally, data show that the ROCK inhibitor (Y-27632) reduces the small intestinal permeability in everted sacs of young mice, pointing out the purpose of the Rho kinase (ROCK) signalling cascade in the intestinal permeability alteration. Results of the present study suggest that a dysregulation of NO synthesis probably has a result of an increased activity of arginase, which is critical in the dysregulation of intestinal barrier in aging mice. However, more research is required to better understand the mechanism of the analysed signal path and address this aspect in future. Upcoming studies should take into consideration the two coexisting arginase isoforms, type 1 predominantly expressed in the liver and type 2 expressed throughout extrahepatic tissues [151], and therefore, perform experiments including potential inhibitors sensitive to each arginase subtype. RNA knockdown strategies have been suggested to specifically downregulate the expression of a single arginase type, due to the lack of isotype-selective, cell-targeted inhibitors [155]. The effects of arginase inhibitors in larger clinical settings, the pharmacokinetic and toxicological factors, as well as the potential adverse effects in long-term treatments remain to be determined [156]. Researchers should additionally perform assays to determinate the arginase activity [157] to obtain a better insight of its role in the NO metabolism and intestinal barrier dysfunction. On the other hand, there are still several open questions present in the tight junction research that need to be addressed [153]. It has to be further investigated how the increased arginase activity regulates the tight junction proteins and via which molecular mechanisms [154]. Gut microbiota are an additional key factor influencing the efficient development and maintenance of the intestinal barrier and should be taken into account [152]. The microbiota synthesizes a great array of metabolites in the intestine, which generate the micro-environment crucial to defining the mechanism of diseases and progress of potential therapeutics [158].

Moreover, commensal intestinal bacteria can have beneficial effects on the physiology of the epithelial permeability, especially on tight junction repair and maintenance [159]. Furthermore, the study by Višnjić et al. (2021) is warning AICAR-based studies in the interpretation of the AMPK signalling pathway, since the modulator of AMPK activity may have several AMPK-independent effects and more complex models of AMPK downregulation and knockout are being introduced [160]. In addition, researchers should focus on the poor oral bioavailability AICAR has shown in clinical trials and find the preferred route of administration for the aimed patient group [161]. Concluding, perspectives of inhibiting arginase activity hold therapeutical potential for improving intestinal barrier function and decreasing the prevalence of GI diseases in the elderly population, leading to an ameliorated lifespan and reduction of the major source of morbidity, mortality, and healthcare costs.

7. Summary

Due to a worldwide increase in life expectancy, the proportion of elderly in the global population continues to rise. However, while overall life expectancy is increasing, the 'healthy life span' is not increasing accordingly. An intact intestinal barrier is central to human nutrition, health, and wellbeing and therefore possibly also for healthy aging. Unpublished data of the own working group show an increased intestinal arginase activity in aged rodents, alongside an intestinal barrier dysfunction. Based on this background, this study aimed to determine if a dysfunction of the nitric oxide (NO) metabolism is critical in aging associated decline of intestinal barrier function. Specifically, the effect of arginase inhibitor nor-NOHA (N-ω-Hydroxy-L-norarginine) on the messenger ribonucleic acid (mRNA) expression of tight junction (TJ) proteins occludin and zonula-occludens-1 (ZO-1) and marker of senescence HMGB1 in proximal small intestinal tissue of young (3mo) and old (17mo) mice was analysed with a real-time qPCR. Permeation of D-xylose was measured in everted sacs bult from small intestinal tissue of young (5mo) and old (22-23mo) mice to detect changes due to modulating: arginase activity, rho-associated protein kinase (ROCK) signalling cascade and adenosine monophosphate-activated protein kinase (AMPK)-related signalling cascade. Additionally, Western blot analysis was performed to determine if the treatment with nor-NOHA, AICAR (5-aminoimidazole-4-carboxamide riboside) or Y-27632 (ROCK inhibitor) affects the occludin, myosin light-chain kinase, β-actin and phospho-occludin concentration in small intestinal tissue of young (5mo) and old (22-23mo) mice. The results of the present study indicate that the arginase inhibitor nor-NOHA significantly upregulates the occludin and ZO-1 mRNA expression in small intestinal tissue of old mice compared to vehicle treated mice. Furthermore, treatment with nor-NOHA is associated with a higher HMGB1 mRNA expression in aged small intestinal tissue. The direct AMPK activator AICAR and the ROCK inhibitor Y-27632 reduced the D-xylose permeation in everted small intestinal tissue sacs of young and old mice compared to control. Moreover, everted sacs of aged animals incubated with Y-27632 showed lower ratio of phospho-occludin to total occludin. In conclusion, results of the present study suggest that a dysregulation of NO synthesis, possibly as a result of an increased activity of arginase, maybe critical in the development of age-associated intestinal barrier dysfunction. However, future studies will have to address this in more detail.

8. Zusammenfassung

Aufgrund der weltweit steigenden Lebenserwartung erhöht sich der Anteil älterer Menschen an der Weltbevölkerung weiter an. Während jedoch die Gesamtlebenserwartung steigt, nimmt die „gesunde Lebensspanne“ nicht entsprechend zu. Eine intakte Darmbarriere ist zentral für die menschliche Ernährung, Gesundheit und das Wohlbefinden und damit möglicherweise auch für ein gesundes Altern. Unveröffentlichte Daten der eigenen Arbeitsgruppe zeigen eine erhöhte intestinale Arginase-Aktivität bei gealterten Nagern neben einer Darmbarriere-Dysfunktion. Basierend auf diesem Hintergrund sollte in dieser Studie untersucht werden, ob eine Dysfunktion des Stickstoffmonoxid-(NO)-Stoffwechsels entscheidend für den altersbedingten Rückgang der Darmbarrierefunktion ist. Wirkung des Arginasehemmers nor-NOHA (N-ω-Hydroxy-L-norarginine) auf die Messenger-Ribonukleinsäure(mRNA)-Expression der Tight Junction(TJ)-Proteine Occludin und Zonula-Occludens-1 (ZO-1) und der Seneszenzmarker HMGB1, im proximalen Dünndarmgewebe von jungen (3mo) und alten (17mo) Mäusen, wurde mit einer real-time qPCR analysiert. Die Permeation von D-Xylose wurde in everted sacs aus Dünndarmgewebe junger (5 Monate) und alter (22-23 Monate) Mäuse gemessen, um Veränderungen aufgrund der Modulation von: Arginaseaktivität, Rho-assoziierte Proteinkinase (ROCK) Signalkaskade und Adenosin Monophosphat-aktivierte Proteinkinase (AMPK)-verwandte Signalkaskade, zu erkennen. Darüber hinaus wurde eine Western-Blot-Analyse durchgeführt, um festzustellen, ob die Behandlung mit nor-NOHA, AICAR (5-aminoimidazole-4-carboxamide riboside) oder Y-27632 (ROCK-Inhibitor) die Konzentration von Occludin, Myosin light-chain kinase, β-Actin and Phospho-Occludin im Dünndarmgewebe von jungen (5mo) und alten (22-23mo) Mäusen beeinflusst. Die Ergebnisse der vorliegenden Studie zeigen, dass der Arginase-Inhibitor nor-NOHA die Occludin- und ZO1-mRNA-Expression im Dünndarmgewebe alter Mäuse im Vergleich zu mit Vehikel behandelten Mäusen signifikant hochreguliert. Darüber hinaus ist die Behandlung mit nor-NOHA mit einer höheren HMGB1-mRNA-Expression in gealtertem Dünndarmgewebe verbunden. Der direkte AMPK-Aktivator AICAR und der ROCK-Inhibitor Y-27632 reduzierten die D-Xylose-Permeation in everted sacs junger und alter Mäuse im Vergleich zur Kontrolle. Außerdem zeigten everted sacs von gealterten Tieren, die mit Y-27632 inkubiert wurden, ein niedrigeres Verhältnis von Phospho-Occludin zu Gesamt-Occludin. Zusammenfassend legen die Ergebnisse der vorliegenden Studie nahe, dass eine Fehlregulation der NO-Synthese, möglicherweise als Folge einer erhöhten Aktivität der Arginase, entscheidend für die Entwicklung einer altersbedingten Darmbarriere-Dysfunktion ist. Zukünftige Studien müssen sich jedoch genauer damit befassen.

A. References

[1] De Winter G. Aging as disease. Med Health Care Philos. 2015 May;18(2):237-43. doi: 10.1007/s11019-014-9600-y. PMID: 25240472.

[2] Partridge L, Deelen J, Slagboom PE. Facing up to the global challenges of ageing. Nature. 2018 Sep;561(7721):45-56. doi: 10.1038/s41586-018-0457-8. Epub 2018 Sep 5. PMID: 30185958.

[3] McLean AJ, Le Couteur DG. Aging biology and geriatric clinical pharmacology. Pharmacol Rev. 2004 Jun;56(2):163-84. doi: 10.1124/pr.56.2.4. PMID: 15169926.

[4] United Nations, Department of Economic and Social Affairs, Population Division (2019). World Population Ageing 2019: Highlights (ST/ESA/SER.A/430).

[5] World Health Organisation (WHO), (2018, February 5). Ageing and health. Retrieved Novem-ber 25, 2020, from https://www.who.int/news-room/fact-sheets/detail/ageing-and-health

[6] Liu, Z., Kuo, P. L., Horvath, S., Crimmins, E., Ferrucci, L., & Levine, M. (2018). A new aging measure captures morbidity and mortality risk across diverse subpopulations from NHANES IV: A cohort study. PLoS medicine, 15(12), e1002718. https://doi.org/10.1371/journal.pmed.1002718

[7] Gao, T., Wang, X. C., Chen, R., Ngo, H. H., & Guo, W. (2015). Disability adjusted life year (DALY): a useful tool for quantitative assessment of environmental pollution. The Science of the total environment, 511, 268–287. https://doi.org/10.1016/j.scitotenv.2014.11.048

[8] Eurostat Database (2020, April 6). Healthy life years statistics - Statistics Explained. Retrieved November 25, 2020, from https://ec.europa.eu/eurostat/statistics-explained/index.php/Healthy_life_years_statistics#:~:text=years%20at%20birth-,In%202018%2C%20the%20number%20of%20healthy%20life%20years%20at%20birth,men%20in%20the%20EU%2D27.&text=Life%20expectancy%20for%20women%20in,be%20lived%20with%20activity%20limitations.

[9] Campisi J, Kapahi P, Lithgow GJ, Melov S, Newman JC, Verdin E. From discoveries in age-ing research to therapeutics for healthy ageing. Nature. 2019 Jul;571(7764):183-192. doi: 10.1038/s41586-019-1365-2. Epub 2019 Jul 10. PMID: 31292558; PMCID: PMC7205183.

[10] Lee JJ, Park IH, Rhee WJ, Kim HS, Shin JS. HMGB1 modulates the balance between senescence and apoptosis in response to genotoxic stress. FASEB J. 2019 Oct;33(10):10942-10953. doi: 10.1096/fj.201900288R. Epub 2019 Jul 5. PMID: 31284735.

[11] Davalos AR, Kawahara M, Malhotra GK, Schaum N, Huang J, Ved U, Beausejour CM, Coppe JP, Rodier F, Campisi J. p53-dependent release of Alarmin HMGB1 is a central

mediator of senescent phenotypes. J Cell Biol. 2013 May 13;201(4):613-29. doi: 10.1083/jcb.201206006. Epub 2013 May 6. PMID: 23649808; PMCID: PMC3653366.

[12] Schmeer C, Kretz A, Wengerodt D, Stojiljkovic M, Witte OW. Dissecting Aging and Senescence-Current Concepts and Open Lessons. Cells. 2019 Nov 15;8(11):1446. doi: 10.3390/cells8111446. PMID: 31731770; PMCID: PMC6912776.

[13] Soenen, S., Rayner, C. K., Jones, K. L., & Horowitz, M. (2016). The ageing gastrointestinal tract. Current opinion in clinical nutrition and metabolic care, 19(1), 12–18. https://doi.org/10.1097/MCO.0000000000000238

[14] Drozdowski, L., & Thomson, A. B. (2006). Aging and the intestine. World journal of gastroen-terology, 12(47), 7578–7584. https://doi.org/10.3748/wjg.v12.i47.7578

[15] Durazzo, M., Campion, D., Fagoonee, S., & Pellicano, R. (2017). Gastrointestinal tract disor-ders in the elderly. Minerva medica, 108(6), 575–591. https://doi.org/10.23736/S0026-4806.17.05417-9

[16] Holt P. R. (2003). Gastrointestinal diseases in the elderly. Current opinion in clinical nutrition and metabolic care, 6(1), 41–48. https://doi.org/10.1097/00075197-200301000-00007

[17] Agarwal, E., Miller, M., Yaxley, A., & Isenring, E. (2013). Malnutrition in the elderly: a narra-tive review. Maturitas, 76(4), 296–302. https://doi.org/10.1016/j.maturitas.2013.07.013

[18] Man AL, Bertelli E, Rentini S, Regoli M, Briars G, Marini M, Watson AJ, Nicoletti C. Age-associated modifications of intestinal permeability and innate immunity in human small intestine. Clin Sci (Lond). 2015 Oct;129(7):515-27. doi: 10.1042/CS20150046. Epub 2015 May 7. PMID: 25948052.

[19] Greenwood-Van Meerveld, B., Johnson, A. C., & Grundy, D. (2017). Gastrointestinal Physi-ology and Function. Handbook of experimental pharmacology, 239, 1–16. https://doi.org/10.1007/164_2016_118

[20] Johnstone, C., Hendry, C., Farley, A., & McLafferty, E. (2014). The digestive system: part 1. Nursing standard (Royal College of Nursing (Great Britain) : 1987), 28(24), 37–45. https://doi.org/10.7748/ns2014.02.28.24.37.e7395

[21] Volk, N., & Lacy, B. (2017). Anatomy and Physiology of the Small Bowel. Gastrointestinal endoscopy clinics of North America, 27(1), 1–13. https://doi.org/10.1016/j.giec.2016.08.001

[22] Ahluwalia, B., Magnusson, M. K., & Öhman, L. (2017). Mucosal immune system of the gas-trointestinal tract: maintaining balance between the good and the bad. Scandinavian journal of gastroenterology, 52(11), 1185–1193. https://doi.org/10.1080/00365521.2017.1349173

[23] Allaire, J. M., Crowley, S. M., Law, H. T., Chang, S. Y., Ko, H. J., & Vallance, B. A. (2018). The Intestinal Epithelium: Central Coordinator of Mucosal Immunity. Trends in immunology, 39(9), 677–696. https://doi.org/10.1016/j.it.2018.04.002

[24] Boland M. (2016). Human digestion--a processing perspective. Journal of the science of food and agriculture, 96(7), 2275–2283. https://doi.org/10.1002/jsfa.7601

[25] Takiishi, T., Fenero, C., & Câmara, N. (2017). Intestinal barrier and gut microbiota: Shaping our immune responses throughout life. Tissue barriers, 5(4), e1373208. https://doi.org/10.1080/21688370.2017.1373208

[26] Caricilli, A. M., Castoldi, A., & Câmara, N. O. (2014). Intestinal barrier: A gentlemen's agreement between microbiota and immunity. World journal of gastrointestinal pathophysiology, 5(1), 18–32. https://doi.org/10.4291/wjgp.v5.i1.18

[27] Rooks, M. G., & Garrett, W. S. (2016). Gut microbiota, metabolites and host immunity. Na-ture reviews. Immunology, 16(6), 341–352. https://doi.org/10.1038/nri.2016.42

[28] König, J., Wells, J., Cani, P. D., García-Ródenas, C. L., MacDonald, T., Mercenier, A., Whyte, J., Troost, F., & Brummer, R. J. (2016). Human Intestinal Barrier Function in Health and Disease. Clinical and translational gastroenterology, 7(10), e196. https://doi.org/10.1038/ctg.2016.54

[29] Lerner, A., & Matthias, T. (2015). Changes in intestinal tight junction permeability associated with industrial food additives explain the rising incidence of autoimmune disease. Autoimmunity reviews, 14(6), 479–489. https://doi.org/10.1016/j.autrev.2015.01.009

[30] Lee, B., Moon, K. M., & Kim, C. Y. (2018). Tight Junction in the Intestinal Epithelium: Its As-sociation with Diseases and Regulation by Phytochemicals. Journal of immunology research, 2018, 2645465. https://doi.org/10.1155/2018/2645465

[31] He, C., Yu, T., Shi, Y., Ma, C., Yang, W., Fang, L., Sun, M., Wu, W., Xiao, F., Guo, F., Chen, M., Yang, H., Qian, J., Cong, Y., & Liu, Z. (2017). MicroRNA 301A Promotes Intestinal Inflamma-tion and Colitis-Associated Cancer Development by Inhibiting BTG1. Gastroenterology, 152(6), 1434–1448.e15. https://doi.org/10.1053/j.gastro.2017.01.049

[32] Araújo, J. R., Tomas, J., Brenner, C., & Sansonetti, P. J. (2017). Impact of high-fat diet on the intestinal microbiota and small intestinal physiology before and after the onset of obesity. Bio-chimie, 141, 97–106. https://doi.org/10.1016/j.biochi.2017.05.019

[33] Köhler, C. A., Maes, M., Slyepchenko, A., Berk, M., Solmi, M., Lanctôt, K. L., & Carvalho, A. F. (2016). The Gut-Brain Axis, Including the Microbiome, Leaky Gut and Bacterial Translocation: Mechanisms and Pathophysiological Role in Alzheimer's Disease. Current pharmaceutical de-sign, 22(40), 6152–6166. https://doi.org/10.2174/1381612822666160907093807

[34] Camara-Lemarroy, C. R., Metz, L., Meddings, J. B., Sharkey, K. A., & Wee Yong, V. (2018). The intestinal barrier in multiple sclerosis: implications for pathophysiology and therapeutics. Brain : a journal of neurology, 141(7), 1900–1916. https://doi.org/10.1093/brain/awy131

[35] Drozdowski, L., & Thomson, A. B. (2006). Aging and the intestine. World journal of gastroen-terology, 12(47), 7578–7584. https://doi.org/10.3748/wjg.v12.i47.7578

[36] Ren, W. Y., Wu, K. F., Li, X., Luo, M., Liu, H. C., Zhang, S. C., & Hu, Y. (2014). Age-related changes in small intestinal mucosa epithelium architecture and epithelial tight junction in rat models. Aging clinical and experimental research, 26(2), 183–191. https://doi.org/10.1007/s40520-013-0148-0

[37] Steegenga, W. T., de Wit, N. J., Boekschoten, M. V., Ijssennagger, N., Lute, C., Keshtkar, S., Bromhaar, M. M., Kampman, E., de Groot, L. C., & Muller, M. (2012). Structural, functional and molecular analysis of the effects of aging in the small intestine and colon of C57BL/6J mice. BMC medical genomics, 5, 38. https://doi.org/10.1186/1755-8794-5-38

[38] Nandagopalan, P. A., Magdalene, K. F., & Binu, A. (2014). Effect of Aging on the Quantita-tive Number of Brunner's Glands. Journal of clinical and diagnostic research : JCDR, 8(3), 4–6. https://doi.org/10.7860/JCDR/2014/7652.4087

[39] Strugari, A., Stan, M. S., Gharbia, S., Hermenean, A., & Dinischiotu, A. (2018). Characteriza-tion of Nanoparticle Intestinal Transport Using an In Vitro Co-Culture Model. Nanomaterials (Ba-sel, Switzerland), 9(1), 5. https://doi.org/10.3390/nano9010005

[40] Buckley, A., & Turner, J. R. (2018). Cell Biology of Tight Junction Barrier Regulation and Mucosal Disease. Cold Spring Harbor perspectives in biology, 10(1), a029314. https://doi.org/10.1101/cshperspect.a029314

[41] Dumic, I., Nordin, T., Jecmenica, M., Stojkovic Lalosevic, M., Milosavljevic, T., & Milovanov-ic, T. (2019). Gastrointestinal Tract Disorders in Older Age. Canadian journal of gastroenterology & hepatology, 2019, 6757524. https://doi.org/10.1155/2019/6757524

[42] Tran, L., & Greenwood-Van Meerveld, B. (2013). Age-associated remodeling of the intestinal epithelial barrier. The journals of gerontology. Series A, Biological sciences and medical scienc-es, 68(9), 1045–1056. https://doi.org/10.1093/gerona/glt106

[43] Ren, W. Y., Wu, K. F., Li, X., Luo, M., Liu, H. C., Zhang, S. C., & Hu, Y. (2014). Age-related changes in small intestinal mucosa epithelium architecture and epithelial tight junction in rat models. Aging clinical and experimental research, 26(2), 183–191. https://doi.org/10.1007/s40520-013-0148-0

[44] Ponnappan, S., & Ponnappan, U. (2011). Aging and immune function: molecular mecha-nisms to interventions. Antioxidants & redox signaling, 14(8), 1551–1585. https://doi.org/10.1089/ars.2010.3228

[45] Liguori, I., Russo, G., Curcio, F., Bulli, G., Aran, L., Della-Morte, D., Gargiulo, G., Testa, G., Cacciatore, F., Bonaduce, D., & Abete, P. (2018). Oxidative stress, aging, and diseases. Clinical interventions in aging, 13, 757–772. https://doi.org/10.2147/CIA.S158513

[46] Julio-Pieper, M., & Bravo, J. A. (2016). Intestinal Barrier and Behavior. International review of neurobiology, 131, 127–141. https://doi.org/10.1016/bs.irn.2016.08.006

[47] Valentini, L., Ramminger, S., Haas, V., Postrach, E., Werich, M., Fischer, A., Koller, M., Swidsinski, A., Bereswill, S., Lochs, H., & Schulzke, J. D. (2014). Small intestinal permeability in older adults. Physiological reports, 2(4), e00281. https://doi.org/10.14814/phy2.281

[48] Soeters, P. B., Luyer, M. D., Greve, J. W., & Buurman, W. A. (2007). The significance of bowel permeability. Current opinion in clinical nutrition and metabolic care, 10(5), 632–638. https://doi.org/10.1097/MCO.0b013e3282a0780e

[49] Farré, R., Fiorani, M., Abdu Rahiman, S., & Matteoli, G. (2020). Intestinal Permeability, In-flammation and the Role of Nutrients. Nutrients, 12(4), 1185. https://doi.org/10.3390/nu12041185

[50] Crosnier, C., Stamataki, D., & Lewis, J. (2006). Organizing cell renewal in the intestine: stem cells, signals and combinatorial control. Nature reviews. Genetics, 7(5), 349–359. https://doi.org/10.1038/nrg1840

[51] Kiela, P. R., & Ghishan, F. K. (2009). Ion transport in the intestine. Current opinion in gastro-enterology, 25(2), 87–91. https://doi.org/10.1097/MOG.0b013e3283260900

[52] Clayburgh, D. R., Shen, L., & Turner, J. R. (2004). A porous defense: the leaky epithelial barrier in intestinal disease. Laboratory investigation; a journal of technical methods and patholo-gy, 84(3), 282–291. https://doi.org/10.1038/labinvest.3700050

[53] Suzuki T. (2013). Regulation of intestinal epithelial permeability by tight junctions. Cellular and molecular life sciences : CMLS, 70(4), 631–659. https://doi.org/10.1007/s00018-012-1070-x

[54] Camilleri M. (2019). Leaky gut: mechanisms, measurement and clinical implications in hu-mans. Gut, 68(8), 1516–1526. https://doi.org/10.1136/gutjnl-2019-318427

[55] Odenwald, M. A., & Turner, J. R. (2013). Intestinal permeability defects: is it time to treat?. Clinical gastroenterology and hepatology : the official clinical practice journal of the American Gastroenterological Association, 11(9), 1075–1083. https://doi.org/10.1016/j.cgh.2013.07.001

[56] Leech, B., McIntyre, E., Steel, A., & Sibbritt, D. (2019). Risk factors associated with intestinal permeability in an adult population: A systematic review. International journal of clinical practice, 73(10), e13385. https://doi.org/10.1111/ijcp.13385

[57] Galipeau, H. J., & Verdu, E. F. (2016). The complex task of measuring intestinal permeability in basic and clinical science. Neurogastroenterology and motility : the official journal of the Euro-pean Gastrointestinal Motility Society, 28(7), 957–965. https://doi.org/10.1111/nmo.12871

[58] Lanas A. (2008). Role of nitric oxide in the gastrointestinal tract. Arthritis research & therapy, 10 Suppl 2(Suppl 2), S4. https://doi.org/10.1186/ar2465

[59] Shah, V., Lyford, G., Gores, G., & Farrugia, G. (2004). Nitric oxide in gastrointestinal health and disease. Gastroenterology, 126(3), 903–913. https://doi.org/10.1053/j.gastro.2003.11.046

[60] Cho C. H. (2001). Current roles of nitric oxide in gastrointestinal disorders. Journal of physi-ology, Paris, 95(1-6), 253–256. https://doi.org/10.1016/s0928-4257(01)00034-1

[61] Takahashi T. (2003). Pathophysiological significance of neuronal nitric oxide synthase in the gastrointestinal tract. Journal of gastroenterology, 38(5), 421–430. https://doi.org/10.1007/s00535-003-1094-y

[62] Caldwell, R. W., Rodriguez, P. C., Toque, H. A., Narayanan, S. P., & Caldwell, R. B. (2018). Arginase: A Multifaceted Enzyme Important in Health and Disease. Physiological reviews, 98(2), 641–665. https://doi.org/10.1152/physrev.00037.2016

[63] Ash D. E. (2004). Structure and function of arginases. The Journal of nutrition, 134(10 Suppl), 2760S–2767S. https://doi.org/10.1093/jn/134.10.2760S

[64] Yang, Z., & Ming, X. F. (2014). Functions of arginase isoforms in macrophage inflammatory responses: impact on cardiovascular diseases and metabolic disorders. Frontiers in immunology, 5, 533. https://doi.org/10.3389/fimmu.2014.00533

[65] Berkowitz, D. E., White, R., Li, D., Minhas, K. M., Cernetich, A., Kim, S., Burke, S., Shoukas, A. A., Nyhan, D., Champion, H. C., & Hare, J. M. (2003). Arginase reciprocally regulates nitric oxide synthase activity and contributes to endothelial dysfunction in aging blood vessels. Circula-tion, 108(16), 2000–2006. https://doi.org/10.1161/01.CIR.0000092948.04444.C7

[66] Wang, W. W., Qiao, S. Y., & Li, D. F. (2009). Amino acids and gut function. Amino acids, 37(1), 105–110. https://doi.org/10.1007/s00726-008-0152-4

[67] Viana, M. L., Santos, R. G., Generoso, S. V., Arantes, R. M., Correia, M. I., & Cardoso, V. N. (2010). Pretreatment with arginine preserves intestinal barrier integrity and reduces bacterial translocation in mice. Nutrition (Burbank, Los Angeles County, Calif.), 26(2), 218–223. https://doi.org/10.1016/j.nut.2009.04.005

[68] Ren, W., Chen, S., Yin, J., Duan, J., Li, T., Liu, G., Feng, Z., Tan, B., Yin, Y., & Wu, G. (2014). Dietary arginine supplementation of mice alters the microbial population and activates intestinal innate immunity. The Journal of nutrition, 144(6), 988–995. https://doi.org/10.3945/jn.114.192120

[69] Ersin, S., Tuncyurek, P., Esassolak, M., Alkanat, M., Buke, C., Yilmaz, M., Telefoncu, A., & Kose, T. (2000). The prophylactic and therapeutic effects of glutamine- and arginine-enriched diets on radiation-induced enteritis in rats. The Journal of surgical research, 89(2), 121–125. https://doi.org/10.1006/jsre.1999.5808

[70] Schleiffer, R., & Raul, F. (1996). Prophylactic administration of L-arginine improves the intes-tinal barrier function after mesenteric ischaemia. Gut, 39(2), 194–198. https://doi.org/10.1136/gut.39.2.194

[71] Caldwell, R. B., Toque, H. A., Narayanan, S. P., & Caldwell, R. W. (2015). Arginase: an old enzyme with new tricks. Trends in pharmacological sciences, 36(6), 395–405. https://doi.org/10.1016/j.tips.2015.03.006

[72] Pudlo, M., Demougeot, C., & Girard-Thernier, C. (2017). Arginase Inhibitors: A Rational Approach Over One Century. Medicinal research reviews, 37(3), 475–513. https://doi.org/10.1002/med.21419

[73] Xia, Z., Huang, L., Yin, P., Liu, F., Liu, Y., Zhang, Z., Lin, J., Zou, W., & Li, C. (2019). L-Arginine alleviates heat stress-induced intestinal epithelial barrier damage by promoting expres-sion of tight junction proteins via the AMPK pathway. Molecular biology reports, 46(6), 6435–6451. https://doi.org/10.1007/s11033-019-05090-1

[74] Rowart P, Wu J, Caplan MJ, Jouret F (2018) Implications of AMPK in the formation of epithe-lial tight junctions. Int J Mol Sci 19(7):E2040. https://doi.org/10.3390/ijms19072040

[75] Steinberg, G. R., & Kemp, B. E. (2009). AMPK in Health and Disease. Physiological reviews, 89(3), 1025–1078. https://doi.org/10.1152/physrev.00011.2008

[76] Zhu, M. J., Sun, X., & Du, M. (2018). AMPK in regulation of apical junctions and barrier func-tion of intestinal epithelium. Tissue barriers, 6(2), 1–13. https://doi.org/10.1080/21688370.2018.1487249

[77] Kim, J., Yang, G., Kim, Y., Kim, J., & Ha, J. (2016). AMPK activators: mechanisms of action and physiological activities. Experimental & molecular medicine, 48(4), e224. https://doi.org/10.1038/emm.2016.16

[78] Varasteh, S., Braber, S., Kraneveld, A. D., Garssen, J., & Fink-Gremmels, J. (2018). l-Arginine supplementation prevents intestinal epithelial barrier breakdown under heat stress con-ditions by promoting nitric oxide synthesis. Nutrition research (New York, N.Y.), 57, 45–55. https://doi.org/10.1016/j.nutres.2018.05.007

[79] Hopkins AM, Li D, Mrsny RJ, Walsh SV, Nusrat A. Modulation of tight junction function by G protein-coupled events. Adv Drug Deliv Rev 2000;41:329–340.

[80] Amano M, Ito M, Kimura K, Fukata Y, Chihara K, Nakano T, Matsuura Y, Kaibuchi K. Phos-phorylation and activation of myosin by Rho-associated kinase (Rho-kinase). J Biol Chem 1996; 271:20246–20249.

[81] Walsh, S. V., Hopkins, A. M., Chen, J., Narumiya, S., Parkos, C. A., & Nusrat, A. (2001). Rho kinase regulates tight junction function and is necessary for tight junction assembly in polar-ized intestinal epithelia. Gastroenterology, 121(3), 566–579. https://doi.org/10.1053/gast.2001.27060

[82] Dumic, I., Nordin, T., Jecmenica, M., Stojkovic Lalosevic, M., Milosavljevic, T., & Milovanov-ic, T. (2019). Gastrointestinal Tract Disorders in Older Age. Canadian journal of gastroenterology & hepatology, 2019, 6757524. https://doi.org/10.1155/2019/6757524

[83] Valentini, L., Ramminger, S., Haas, V., Postrach, E., Werich, M., Fischer, A., Koller, M., Swidsinski, A., Bereswill, S., Lochs, H., & Schulzke, J. D. (2014). Small intestinal permeability in older adults. Physiological reports, 2(4), e00281. https://doi.org/10.14814/phy2.281

[84] Moretto, J., Girard, C., & Demougeot, C. (2019). The role of arginase in aging: A systematic review. Experimental gerontology, 116, 54–73. https://doi.org/10.1016/j.exger.2018.12.011

[85] World Health Organization. Aging; overview. Retrieved March 1, 2021, from https://www.who.int/health-topics/ageing

[86] Williams, G., Cylus, J., Roubal, T., Ong, P., & Barber, S., SUSTAINABLE HEALTH FINANCING WITH AN AGEING POPULATION; Will population ageing lead to uncontrolled health expenditure growth? The Economics of Healthy and Active Ageing Series. Retrieved March 1, 2021, from https://apps.who.int/iris/bitstream/handle/10665/329382/Policy-brief-1997-8073-2019-3-eng.pdf

[87] López-Otín, C., Blasco, M. A., Partridge, L., Serrano, M., & Kroemer, G. (2013). The hall-marks of aging. Cell, 153(6), 1194–1217. https://doi.org/10.1016/j.cell.2013.05.039

[88] Kirkland J. L. (2016). Translating the Science of Aging into Therapeutic Interventions. Cold Spring Harbor perspectives in medicine, 6(3), a025908. https://doi.org/10.1101/cshperspect.a025908

[89] Kirkland, J. L., & Tchkonia, T. (2017). Cellular Senescence: A Translational Perspective. EBioMedicine, 21, 21–28. https://doi.org/10.1016/j.ebiom.2017.04.013

[90] Bevölkerung nach Alter und Geschlecht. STATISTIK AUSTRIA. Retrieved March 2, 2021, from https://www.statistik.at/web_de/statistiken/menschen_und_gesellschaft/bevoelkerung/bevoelkerungsstruktur/bevoelkerung_nach_alter_geschlecht/index.html

[91] Schwiertz, A., Spiegel, J., Dillmann, U., Grundmann, D., Bürmann, J., Faßbender, K., Schäfer, K. H., & Unger, M. M. (2018). Fecal markers of intestinal inflammation and intestinal permeability are elevated in Parkinson's disease. Parkinsonism & related disorders, 50, 104–107. https://doi.org/10.1016/j.parkreldis.2018.02.022

[92] Stevens, B. R., Goel, R., Seungbum, K., Richards, E. M., Holbert, R. C., Pepine, C. J., & Raizada, M. K. (2018). Increased human intestinal barrier permeability plasma biomarkers zonu-lin and FABP2 correlated with plasma LPS and altered gut microbiome in anxiety or depression. Gut, 67(8), 1555–1557. https://doi.org/10.1136/gutjnl-2017-314759

[93] Rera, M., Clark, R. I., & Walker, D. W. (2012). Intestinal barrier dysfunction links metabolic and inflammatory markers of aging to death in Drosophila. Proceedings of the National Academy of Sciences of the United States of America, 109(52), 21528–21533. https://doi.org/10.1073/pnas.1215849110

[94] Furuse M. (2010). Molecular basis of the core structure of tight junctions. Cold Spring Harbor perspectives in biology, 2(1), a002907. https://doi.org/10.1101/cshperspect.a002907

[95] Branca, J., Gulisano, M., & Nicoletti, C. (2019). Intestinal epithelial barrier functions in age-ing. Ageing research reviews, 54, 100938. https://doi.org/10.1016/j.arr.2019.100938

[96] Shaw, A. C., Goldstein, D. R., & Montgomery, R. R. (2013). Age-dependent dysregulation of innate immunity. Nature reviews. Immunology, 13(12), 875–887. https://doi.org/10.1038/nri3547

[97] Thevaranjan, N., Puchta, A., Schulz, C., Naidoo, A., Szamosi, J. C., Verschoor, C. P., Loukov, D., Schenck, L. P., Jury, J., Foley, K. P., Schertzer, J. D., Larché, M. J., Davidson, D. J., Verdú, E. F., Surette, M. G., & Bowdish, D. (2018). Age-Associated Microbial Dysbiosis Pro-motes Intestinal Permeability, Systemic Inflammation, and Macrophage Dysfunction. Cell host & microbe, 23(4), 570. https://doi.org/10.1016/j.chom.2018.03.006

[98] Liu, A., Lv, H., Wang, H., Yang, H., Li, Y., & Qian, J. (2020). Aging Increases the Severity of Colitis and the Related Changes to the Gut Barrier and Gut Microbiota in Humans and Mice. The journals of gerontology. Series A, Biological sciences and medical sciences, 75(7), 1284–1292. https://doi.org/10.1093/gerona/glz263

[99] Dodig, S., Čepelak, I., & Pavić, I. (2019). Hallmarks of senescence and aging. Biochemia medica, 29(3), 030501. https://doi.org/10.11613/BM.2019.030501

[100] Meier, J., & Sturm, A. (2009). The intestinal epithelial barrier: does it become impaired with age?. Digestive diseases (Basel, Switzerland), 27(3), 240–245. https://doi.org/10.1159/000228556

[101] Bischoff, S. C., Barbara, G., Buurman, W., Ockhuizen, T., Schulzke, J. D., Serino, M., Tilg, H., Watson, A., & Wells, J. M. (2014). Intestinal permeability--a new target for disease prevention and therapy. BMC gastroenterology, 14, 189. https://doi.org/10.1186/s12876-014-0189-7

[102] Gorabi, A. M., Kiaie, N., Hajighasemi, S., Banach, M., Penson, P. E., Jamialahmadi, T., & Sahebkar, A. (2019). Statin-Induced Nitric Oxide Signaling: Mechanisms and Therapeutic Impli-cations. Journal of clinical medicine, 8(12), 2051. https://doi.org/10.3390/jcm8122051

[103] Mirel, L. B., & Carper, K. (2014). Trends in Health Care Expenditures for the Elderly, Age 65 and Older: 2001, 2006, and 2011. In Statistical Brief (Medical Expenditure Panel Survey (US)). Agency for Healthcare Research and Quality (US).

[104] US Department of Health and Human Services (2011). National Institute on Aging - Global health and aging. NIH Publication No.: 11-7737. Retrieved March 15, 2021, from https://www.nia.nih.gov/research/publication/global-health-andaging/preface

[105] Shlisky, J., Bloom, D. E., Beaudreault, A. R., Tucker, K. L., Keller, H. H., Freund-Levi, Y., Fielding, R. A., Cheng, F. W., Jensen, G. L., Wu, D., & Meydani, S. N. (2017). Nutritional Con-siderations for Healthy Aging and Reduction in Age-Related Chronic Disease. Advances in nutri-tion (Bethesda, Md.), 8(1), 17–26. https://doi.org/10.3945/an.116.013474

[106] Wong, R., Ofstedal, M. B., Yount, K., & Agree, E. M. (2008). Unhealthy lifestyles among older adults: exploring transitions in Mexico and the US. European journal of ageing, 5(4), 311–326. https://doi.org/10.1007/s10433-008-0098-0

[107] Muñoz-Espín, D., & Serrano, M. (2014). Cellular senescence: from physiology to pathology. Nature reviews. Molecular cell biology, 15(7), 482–496. https://doi.org/10.1038/nrm3823

[108] Hernandez-Segura, A., Nehme, J., & Demaria, M. (2018). Hallmarks of Cellular Senescence. Trends in cell biology, 28(6), 436–453. https://doi.org/10.1016/j.tcb.2018.02.001

[109] Sharpless, N. E., & Sherr, C. J. (2015). Forging a signature of in vivo senescence. Nature reviews. Cancer, 15(7), 397–408. https://doi.org/10.1038/nrc3960

[110] Lecot, P., Alimirah, F., Desprez, P. Y., Campisi, J., & Wiley, C. (2016). Context-dependent effects of cellular senescence in cancer development. British journal of cancer, 114(11), 1180–1184. https://doi.org/10.1038/bjc.2016.115

[111] Soto-Gamez, A., & Demaria, M. (2017). Therapeutic interventions for aging: the case of cellular senescence. Drug discovery today, 22(5), 786–795. https://doi.org/10.1016/j.drudis.2017.01.004

[112] Johansson, M. E., & Hansson, G. C. (2016). Immunological aspects of intestinal mucus and mucins. Nature reviews. Immunology, 16(10), 639–649. https://doi.org/10.1038/nri.2016.88

[113] Litovchick L. (2020). Staining the Blot for Total Protein with Ponceau S. Cold Spring Harbor protocols, 2020(3), 098459. https://doi.org/10.1101/pdb.prot098459

[114] Camilleri, M., Madsen, K., Spiller, R., Greenwood-Van Meerveld, B., & Verne, G. N. (2012). Intestinal barrier function in health and gastrointestinal disease. Neurogastroenterology and motility : the official journal of the European Gastrointestinal Motility Society, 24(6), 503–512. https://doi.org/10.1111/j.1365-2982.2012.01921.x

[115] Mu, K., Yu, S., & Kitts, D. D. (2019). The Role of Nitric Oxide in Regulating Intestinal Redox Status and Intestinal Epithelial Cell Functionality. International journal of molecular sciences, 20(7), 1755. https://doi.org/10.3390/ijms20071755

[116] Han, X., Fink, M. P., & Delude, R. L. (2003). Proinflammatory cytokines cause NO*-dependent and -independent changes in expression and localization of tight junction proteins in intestinal epithelial cells. Shock (Augusta, Ga.), 19(3), 229–237. https://doi.org/10.1097/00024382-200303000-00006

[117] Biran, A., Zada, L., Abou Karam, P., Vadai, E., Roitman, L., Ovadya, Y., Porat, Z., & Krizhanovsky, V. (2017). Quantitative identification of senescent cells in aging and disease. Aging cell, 16(4), 661–671. https://doi.org/10.1111/acel.12592

[118] McHugh, D., & Gil, J. (2018). Senescence and aging: Causes, consequences, and therapeutic avenues. The Journal of cell biology, 217(1), 65–77. https://doi.org/10.1083/jcb.201708092

[119] González-González, M., Díaz-Zepeda, C., Eyzaguirre-Velásquez, J., González-Arancibia, C., Bravo, J. A., & Julio-Pieper, M. (2019). Investigating Gut Permeability in

Animal Models of Disease. Frontiers in physiology, 9, 1962. https://doi.org/10.3389/fphys.2018.01962

[120] Cynober L. (1994). Can arginine and ornithine support gut functions?. Gut, 35(1 Suppl), S42–S45. https://doi.org/10.1136/gut.35.1_suppl.s42

[121] Rowart, P., Wu, J., Caplan, M. J., & Jouret, F. (2018). Implications of AMPK in the Formation of Epithelial Tight Junctions. International journal of molecular sciences, 19(7), 2040. https://doi.org/10.3390/ijms19072040

[122] Zhu, M. J., Sun, X., & Du, M. (2018). AMPK in regulation of apical junctions and barrier function of intestinal epithelium. Tissue barriers, 6(2), 1–13. https://doi.org/10.1080/21688370.2018.1487249

[123] Grothaus, J. S., Ares, G., Yuan, C., Wood, D. R., & Hunter, C. J. (2018). Rho kinase inhibition maintains intestinal and vascular barrier function by upregulation of occludin in experimental necrotizing enterocolitis. American journal of physiology. Gastrointestinal and liver physiology, 315(4), G514–G528. https://doi.org/10.1152/ajpgi.00357.2017

[124] César Machado, M. C., & da Silva, F. P. (2016). Intestinal Barrier Dysfunction in Human Pathology and Aging. Current pharmaceutical design, 22(30), 4645–4650. https://doi.org/10.2174/1381612822666160510125331

[125] Chen, Y. M., Zhang, J. S., & Duan, X. L. (2003). Changes of microvascular architecture, ultrastructure and permeability of rat jejunal villi at different ages. World journal of gastroenterology, 9(4), 795–799. https://doi.org/10.3748/wjg.v9.i4.795

[126] Elias, B. C., Suzuki, T., Seth, A., Giorgianni, F., Kale, G., Shen, L., Turner, J. R., Naren, A., Desiderio, D. M., & Rao, R. (2009). Phosphorylation of Tyr-398 and Tyr-402 in occludin prevents its interaction with ZO-1 and destabilizes its assembly at the tight junctions. The Journal of biological chemistry, 284(3), 1559–1569. https://doi.org/10.1074/jbc.M804783200

[127] Hamada, K., Shitara, Y., Sekine, S., & Horie, T. (2010). Zonula Occludens-1 alterations and enhanced intestinal permeability in methotrexate-treated rats. Cancer chemotherapy and pharmacology, 66(6), 1031–1038. https://doi.org/10.1007/s00280-010-1253-9

[128] Chen, Y. h., Lu, Q., Schneeberger, E. E., & Goodenough, D. A. (2000). Restoration of tight junction structure and barrier function by down-regulation of the mitogen-activated protein kinase pathway in ras-transformed Madin-Darby canine kidney cells. Molecular biology of the cell, 11(3), 849–862. https://doi.org/10.1091/mbc.11.3.849

[129] Parrish A. R. (2017). The impact of aging on epithelial barriers. Tissue barriers, 5(4), e1343172. https://doi.org/10.1080/21688370.2017.1343172

[130] Xiong, Y., Yepuri, G., Montani, J. P., Ming, X. F., & Yang, Z. (2017). Arginase-II Deficiency Extends Lifespan in Mice. Frontiers in physiology, 8, 682. https://doi.org/10.3389/fphys.2017.00682

[131] Scharl, M., Paul, G., Barrett, K. E., & McCole, D. F. (2009). AMP-activated protein kinase mediates the interferon-gamma-induced decrease in intestinal epithelial barrier function. The Journal of biological chemistry, 284(41), 27952–27963. https://doi.org/10.1074/jbc.M109.046292

[132] Sakakibara, A., Furuse, M., Saitou, M., Ando-Akatsuka, Y., & Tsukita, S. (1997). Possible involvement of phosphorylation of occludin in tight junction formation. The Journal of cell biology, 137(6), 1393–1401. https://doi.org/10.1083/jcb.137.6.1393

[133] Rao R. (2009). Occludin phosphorylation in regulation of epithelial tight junctions. Annals of the New York Academy of Sciences, 1165, 62–68. https://doi.org/10.1111/j.1749-6632.2009.04054.x

[134] Lee S. H. (2015). Intestinal permeability regulation by tight junction: implication on inflammatory bowel diseases. Intestinal research, 13(1), 11–18. https://doi.org/10.5217/ir.2015.13.1.11

[135] Kale, G., Naren, A. P., Sheth, P., & Rao, R. K. (2003). Tyrosine phosphorylation of occludin attenuates its interactions with ZO-1, ZO-2, and ZO-3. Biochemical and biophysical research communications, 302(2), 324–329. https://doi.org/10.1016/s0006-291x(03)00167-0

[136] Atkinson, K. J., & Rao, R. K. (2001). Role of protein tyrosine phosphorylation in acetaldehyde-induced disruption of epithelial tight junctions. American journal of physiology. Gastrointestinal and liver physiology, 280(6), G1280–G1288. https://doi.org/10.1152/ajpgi.2001.280.6.G1280

[137] Meier, J., & Sturm, A. (2009). The intestinal epithelial barrier: does it become impaired with age?. Digestive diseases (Basel, Switzerland), 27(3), 240–245. https://doi.org/10.1159/000228556s

[138] Lovén J, Orlando DA, Sigova AA, Lin CY, Rahl PB, Burge CB, Levens DL, Lee TI, Young RA. Revisiting global gene expression analysis. Cell. 2012 Oct 26;151(3):476-82. doi: 10.1016/j.cell.2012.10.012. PMID: 23101621; PMCID: PMC3505597.

[139] Derveaux S, Vandesompele J, Hellemans J. How to do successful gene expression analysis using real-time PCR. Methods. 2010 Apr;50(4):227-30. doi: 10.1016/j.ymeth.2009.11.001. Epub 2009 Dec 5. PMID: 19969088.

[140] Nwokeoji AO, Kilby PM, Portwood DE, Dickman MJ. Accurate Quantification of Nucleic Acids Using Hypochromicity Measurements in Conjunction with UV Spectrophotometry. Anal Chem. 2017 Dec 19;89(24):13567-13574. doi: 10.1021/acs.analchem.7b04000. Epub 2017 Dec 5. PMID: 29141408.

[141] Tataurov AV, You Y, Owczarzy R. Predicting ultraviolet spectrum of single stranded and double stranded deoxyribonucleic acids. Biophys Chem. 2008 Mar;133(1-3):66-70. doi: 10.1016/j.bpc.2007.12.004. Epub 2007 Dec 23. PMID: 18201813.

[142] Green MR, Sambrook J. Quantification of DNA by Real-Time Polymerase Chain Reaction (PCR). Cold Spring Harb Protoc. 2018 Oct 1;2018(10). doi: 10.1101/pdb.prot095034. PMID: 30275076

[143] Hong Xuan Jin, Seung Bum Seo, Hye Young Lee, Sohee Cho, Jianye Ge, Jonathan King, Bruce Budowle & Soong Deok Lee (2014) Differences of PCR efficiency between two-step PCR and standard three-step PCR protocols in short tandem repeat amplification, Australian Journal of Forensic Sciences, 46:1, 80-90, DOI: 10.1080/00450618.2013.788681

[144] Gadkar Vy, Filion M. New Developments in Quantitative Real-time Polymerase Chain Reaction Technology. Curr Issues Mol Biol. 2014;16:1-6. Epub 2013 Apr 8. PMID: 23562919

[145] Rodriguez-Lazaro D, Hernandez M. Real-time PCR in Food Science: Identification methods. Curr Issues Mol Biol. 2013;15:25-38. Epub 2013 Mar 19. PMID: 23513038.

[146] Green MR, Sambrook J. Analysis and Normalization of Real-Time Polymerase Chain Reaction (PCR) Experimental Data. Cold Spring Harb Protoc. 2018 Oct 1;2018(10). doi: 10.1101/pdb.top095000. PMID: 30275081

[147] Hamilton KL. Even an old technique is suitable in the molecular world of science: the everted sac preparation turns 60 years old. Am J Physiol Cell Physiol. 2014 Apr 15;306(8):C715-20. doi: 10.1152/ajpcell.00041.2014. Epub 2014 Feb 26. PMID: 24573083.

[148] Hamilton KL, Butt AG. Glucose transport into everted sacs of the small intestine of mice. Adv Physiol Educ. 2013 Dec;37(4):415-26. doi: 10.1152/advan.00017.2013. PMID: 24292921.

[149] Antunes DM, da Costa JP, Campos SM, Paschoal PO, Garrido V, Siqueira M, Teixeira GA, Cardoso GP. The serum D-xylose test as a useful tool to identify malabsorption in rats with antigen specific gut inflammatory reaction. Int J Exp Pathol. 2009 Apr;90(2):141-7. doi: 10.1111/j.1365-2613.2008.00627.x. PMID: 19335552; PMCID: PMC2676701.

[150] Julio-Pieper M, Bravo JA. Intestinal Barrier and Behavior. Int Rev Neurobiol. 2016;131:127-141. doi: 10.1016/bs.irn.2016.08.006. Epub 2016 Sep 15. PMID: 27793215.

[151] S Clemente, G., van Waarde, A., F Antunes, I., Dömling, A., & H Elsinga, P. (2020). Arginase as a Potential Biomarker of Disease Progression: A Molecular Imaging Perspective. International journal of molecular sciences, 21(15), 5291. https://doi.org/10.3390/ijms21155291

[152] Alam, A., & Neish, A. (2018). Role of gut microbiota in intestinal wound healing and barrier function. Tissue barriers, 6(3), 1539595. https://doi.org/10.1080/21688370.2018.1539595

[153] Schulzke, J. D., Günzel, D., John, L. J., & Fromm, M. (2012). Perspectives on tight junction research. Annals of the New York Academy of Sciences, 1257, 1–19. https://doi.org/10.1111/j.1749-6632.2012.06485.x

[154] Barekatain, R., Chrystal, P. V., Howarth, G. S., McLaughlan, C. J., Gilani, S., & Nattrass, G. S. (2019). Performance, intestinal permeability, and gene expression of selected tight junction proteins in broiler chickens fed reduced protein diets supplemented with arginine, glutamine, and glycine subjected to a leaky gut model. Poultry science, 98(12), 6761–6771. https://doi.org/10.3382/ps/pez393

[155] Steppan, J., Nyhan, D., & Berkowitz, D. E. (2013). Development of novel arginase inhibitors for therapy of endothelial dysfunction. Frontiers in immunology, 4, 278. https://doi.org/10.3389/fimmu.2013.00278

[156] Ivanenkov, Y. A., & Chufarova, N. V. (2014). Small-molecule arginase inhibitors. Pharmaceutical patent analyst, 3(1), 65–85. https://doi.org/10.4155/ppa.13.75

[157] Corraliza, I. M., Campo, M. L., Soler, G., & Modolell, M. (1994). Determination of arginase activity in macrophages: a micromethod. Journal of immunological methods, 174(1-2), 231–235. https://doi.org/10.1016/0022-1759(94)90027-2

[158] Neish A. S. (2009). Microbes in gastrointestinal health and disease. Gastroenterology, 136(1), 65–80. https://doi.org/10.1053/j.gastro.2008.10.080

[159] Khailova, L., Dvorak, K., Arganbright, K. M., Halpern, M. D., Kinouchi, T., Yajima, M., & Dvorak, B. (2009). Bifidobacterium bifidum improves intestinal integrity in a rat model of necrotizing enterocolitis. American journal of physiology. Gastrointestinal and liver physiology, 297(5), G940–G949. https://doi.org/10.1152/ajpgi.00141.2009

[160] Višnjić, D., Lalić, H., Dembitz, V., Tomić, B., & Smoljo, T. (2021). AICAr, a Widely Used AMPK Activator with Important AMPK-Independent Effects: A Systematic Review. Cells, 10(5), 1095. https://doi.org/10.3390/cells10051095

[161] Dixon, R., Gourzis, J., McDermott, D., Fujitaki, J., Dewland, P., & Gruber, H. (1991). AICA-riboside: safety, tolerance, and pharmacokinetics of a novel adenosine-regulating agent. Journal of clinical pharmacology, 31(4), 342–347. https://doi.org/10.1002/j.1552-4604.1991.tb03715.x

B.Attachment

Buffers and solutions

Table 13: Preparation of 1x TBE buffer for the agarose gel electrophoresis

Substances	Mass
TRIS base	67.2 g/L
Boric acid	59.5 g/L
Ethylenediaminetetraacetic acid (EDTA)	1.36 g/L

Table 14: Preparation of KRH buffer for the incubation of the everted sac models

Substances	Mass
Solution 1	100 mL
Solution 2	100 mL
Solution 3	100 mL
Distilled water	500 mL
adjust pH to	7.4
BSA	2 g
Distilled water	c. 200 mL (until total of 1 L)

Table 15: Composition of the solutions for the preparation of the KRH buffer

	Substances	Mass
Solution 1	1.5 M NaCl	67.2 g/L
	50 mM KCl	3.73 g/L
	12 mM $MgSO_4$	1.44 g/L
	20 mM $CaCl_2$ * H_2O	2.94 g/L
Solution 2	250 mM HEPES	59.5 g/L
Solution 3	10 mM KH_2PO_4	1.36 g/L

Table 16: Preparation of three standard solutions for the D-xylose assay

	D-Xylose	Benzoic acid	Molarity
D-Xylose standard 1	52.5 mg	500 ml	0.7 mM
D-Xylose standard 2	97.6 mg	500 ml	1.3 mM
D-Xylose standard 3	195.2 mg	500 ml	2.6 mM

Table 17: Composition of the RIPA buffer for the total protein isolation

Substances	Concentration
MOPS (3-(N-Morpholino) propan sulfonic acid	20 mM
NaCl	150 mM
EDTA	1 mM
IGEPAL	1 % (v/v)
SDS	0,1 % (w/v)

Table 18: Composition of TRIS 1,5M for the separating SDS-polyacrylamide gel

Substances	Mass
TRIS base	18,15 g
Distilled water	80 mL
adjust pH to	8,8
Distilled water	c. 20 mL (until total of 100mL)

Table 19: Composition of TRIS 0,5M for the stacking SDS-polyacrylamide gel

Substances	Mass
TRIS base	6,05 g
Distilled water	90 mL
adjust pH to	6,8
Distilled water	c. 10 mL (until total of 100mL)

Table 20: Composition of 10% APS for the SDS-polyacrylamide gels

Substances	Mass
Ammonium persulfate	0,1 g
Distilled water	1 mL

Table 21: Composition of 10% SDS for the SDS-polyacrylamide gels

Substances	Mass
Sodium dodecyl sulphate	10 g
Distilled water	100 mL

Table 22: Preparation of the 4x SDS loading buffer for the electrophoresis

Substances	Mass
1,5 M TRIS (pH 6,8)	5.217 mL
SDS	2.5 g
Glycerol	12.5 mL
β-Mercaptoethanol	5 mL
Bromophenol blue	12.5 mg
Aq. des.	until total of 25 mL

Table 23: Preparation of 10x TBS electrophoresis buffer for the protein separation

Substances	Mass
TRIS base	30.28 g
Glycine	144.13 g
SDS	10 g
Distilled water	until total of 1 L

Table 24: Preparation of the Towbin transfer buffer used for Western blotting

Substances	Mass
Glycine	14.4 g
TRIS base	3.03 g
Methanol	200 mL
Distilled water	until total of 1 L
adjust pH to	8.1 – 8.5

Table 25: Preparation of the Ponceau S used for the membrane staining

Substances	Mass
Ponceau S	0,1 g
Acetic acid	500 µL
Distilled water	until total of 50 mL

Table 26: Preparation of the TBST buffer used for the membrane blocking and antibody incubation

Substances	Mass
1x TBS	1 L
Tween 20	500 µL

C. Declaration of independence

I, ...,
declare that I have followed the principles of good scientific practice while writing the present master ‘s thesis:

„ Effect of the arginase inhibitor nor-NOHA on markers of intestinal permeability in aging mice “.

I have written the paper/thesis independently and have used no other sources or aids than those given and have marked the passages taken from other works word-for word or paraphrased.

I furthermore declare that the submitted unencrypted electronic document exactly and without exception corresponds to the contents and wording of the printed copy of the thesis. I give my consent to this electronic version being checked for plagiarism with analytical software.

.....

Place, Date Signature